Check for updates

Received: 23 April 2025 | Revised: 21 August 2025 | Accepted: 8 September 2025

DOI: 10.1002/VIW.20250063

REVIEW

Tissue engineering for tendon and ligament repair: Insights and advances

Francesca Romano[1,2] | **Francesco Lopresti**[1] | **Roberto Di Gesù**[2] | **Vincenzo La Carrubba**[1]

[1]Department of Engineering, University of Palermo, Palermo, Italy

[2]Musculoskeletal Tissue Engineering (MsTE) Laboratory, Ri.MED Foundation, Palermo, Italy

Correspondence
Roberto Di Gesù, Musculoskeletal Tissue Engineering (MsTE) Laboratory, Ri.MED Foundation, Palermo, Italy.
Email: rdigesu@fondazionerimed.com

Funding information
Fondazione Ri.Med

Abstract

Diseases and injuries affecting tendons (Ts) and ligaments (Ls) are among the most frequently diagnosed musculoskeletal disorders. Although many of these are not life threatening, they can cause severe debilitation, ultimately leading to substantial reductions in the patients' mobility and quality of life. Even though the relevant advances in surgical and rehabilitative approaches to treat T/Ls diseases, the incidence of complications associated with those approaches is still too high, making T/Ls diseases an unmet clinical need. Currently, there is no consensus on an effective therapeutic strategy able to promote a complete T/Ls healing process. Over the past decade, there has been a growing interest in developing tissue-engineered T constructs as viable graft alternatives. In this review, we aim to delve into the latest advancements in the field of tissue engineering for T repair. The most advanced technologies such as electrospinning, 3D printing, melt electrowriting, and hybrid fabrication techniques have been discussed, adopting critical connections with biological and biomolecular aspects. Furthermore, this review provides comprehensive insights into current strategies, and future directions, of T/Ls regeneration using tissue engineering approaches, thus paving the way to the development of new effective approaches to T/Ls diseases.

1 | INTRODUCTION

Every year in the United States, about 17 million people suffer from tendon injuries (TIs) and ligament injuries (LIs), needing medical intervention to be repaired. These kinds of injuries significantly impact patients' quality of life, drastically limiting their daily activities, and consequently, negatively influencing their social life. Besides this aspect, it is worth highlighting that TIs/LIs represent a relevant economic burden for medical care, requesting an economic effort that exceeds 40 billion in the United States.[1] TIs/LIs comprehend a plethora of medical conditions including ruptures, overuse injuries, and inflammatory/degenerative conditions such as tendinopathies.[2] The clinical impact of TIs/LIs is intuitively related to the role that tendons and ligaments (Ts/Ls) play in vivo. They act as influential components of the musculotendinous unit by facilitating the transfer of forces from muscles to bones, ultimately allowing the joint movement.[3] Intuitively, joints represent a high-demanding environment in

This is an open access article under the terms of the Creative Commons Attribution License, which permits use, distribution and reproduction in any medium, provided the original work is properly cited.
© 2025 The Author(s). *VIEW* published by Shanghai Fuji Technology Consulting Co., Ltd, authorized by China Professional Community of Experimental Medicine, National Association Health Industry Enterprise Management (CPCEM) and John Wiley & Sons Australia, Ltd.

terms of mechanical solicitation, and this aspect is emphasized in major joints like knee or hip. For this reason, Ts are constitutively more resistant to tensile forces if compared with muscles, supporting up to 17 times the body weight.[4]

Despite their high mechanical resistance, the T/Ls integrity is progressively weakened by the repeated and numerous stresses of daily life, resulting in microtraumas that ultimately lead to ruptures. This process is more evident in structures involved in the most employed joints, such as the Achilles T, which is one of the most frequently injured Ts in the body.[3] Regardless of the T/L involved, each damage represents challenging clinical evidence since both T/Ls have a limited self-healing capability, mainly linked to their hypovascular and hypocellular histological composition.[5]

Currently, surgical approaches represent the elective way to repair TI/LIs after a rupture. However, surgery has relevant drawbacks due to postoperative complications that may lead to chronic pain[6] or hypomotility of the joints.[7] For this reason, different advanced techniques based on tissue engineering (TE) have been developed and successfully applied, either to overcome the postoperative complications or to develop prevention protocols for TI/LI at the early stages.

This review aims to provide an overview of the most recent advances in TE applied to TI/LIs repair, covering a wide range of points of view. We structured the manuscript starting with a general background on T/Ls anatomy, physiology, and biology, as well as on pathologies that often hit T/Ls. Here, we provide information on the importance of T/Ls for the overall musculoskeletal system functionality, underlying how the natural T/Ls self-repair process is unable to regenerate a functional structure after an injury.

Next, we examine a comprehensive section focused on the latest TE approaches adopted to treat TI/LIs. In this section, we deeply analyze the criteria followed to choose the right material as well as the optimal biofabrication technique for each TE application. Furthermore, we provide a clear state-of-the-art on the choice of cells and bioactive molecules, to obtain a scaffold responding to the different needs in T/Ls reconstruction and regeneration, highlighting strengths, and limitations, with a critical approach.

1.1 | T/Ls structure and composition

1.1.1 | Extracellular matrix

Both T/Ls are fibrous and flexible tissues connecting muscles to bones, or bones to bones, respectively. Their primary function is to transfer forces produced by muscles to the adjacent bony structures (Ts) and to stabilize the bone-to-bone interactions (Ls), ultimately allowing complete and cyclic movements around the joints.[5] In terms of both structure and function, Ts/Ls share many similarities.[1,8] Therefore, throughout this review the terms Ts and Ls can be broadly interpreted as referring to both structures. The transitional T-to-bone tissue is histologically complex and is considered as an independent tissue (enthesis) with its own anatomic structure[9], which exhibits a zonal organization transitioning from T (or L) to fibrocartilage, mineralized fibrocartilage, and finally bone. The first layer, primarily composed of fibroblasts and type I collagen, resembles T/L tissue characterized by a highly organized longitudinal collagen alignment. Adjacent to this, the uncalcified fibrocartilage layer contains fibrochondrocytes embedded within a proteoglycan (PG)-rich matrix, with a composition that includes type I–III collagen. The transition to mineralized fibrocartilage is marked by the tidemark, composed of type II collagen, alongside smaller amounts of types I and X collagen, and houses fibrochondrocytes within a mineralized matrix. Finally, the bone layer consists of osteocytes, osteoblasts, and osteoclasts embedded in a mineralized matrix providing a rigid anchorage for T insertion.[10] This gradient of cell types, extracellular matrix (ECM), and mineralization is essential for transmitting forces during movements[11], making T/Ls capable of responding to the high mechanically demanding joints environment. The integration between T/L tissue and bone at the enthesis has its counterpart at the opposite extremity, where Ts connect to muscle fibers. Here, the myotendinous junction (MTJ) serves as the specialized interface that enables the transmission of contractile forces from muscle to T and ultimately to bone. Advanced imaging like transmission electron microscopy, scanning electron microscopy, and focused ion beam microscopy have shown its detailed structure.[12] These methods reveal a complex, interwoven structure where the T's ECM folds into the muscle cell membrane. This design increases the contact area between the tissues, which improves the junction's stability. Muscle projections reach into the T's ECM, forming much of the MTJ and improving tension transfer. Although collagen I and other ECM components are common in the tissue composition of muscle, T, and MTJ, there are distinct differences in the expression of each tissue. For instance, the MTJ is the only location for collagen type XXII, which exhibits interdigitated folding into the muscle fiber membrane to support structural stability and force transmission.[13] The MTJ also features multiple cell types.[14] Tenoblasts and tenocytes maintain the ECM on the T side, while myoblasts and myotubes help form the muscle–T connections. Satellite cells, which are important for muscle repair, are found at the junction and help with regeneration after injury. Endothelial cells assist in

2688268x, 0, Downloaded from https://onlinelibrary.wiley.com/doi/10.1002/VIW.20250063 by CochraneItalia, Wiley Online Library on [16/10/2025]. See the Terms and Conditions (https://onlinelibrary.wiley.com/terms-and-conditions) on Wiley Online Library for rules of use; OA articles are governed by the applicable Creative Commons License

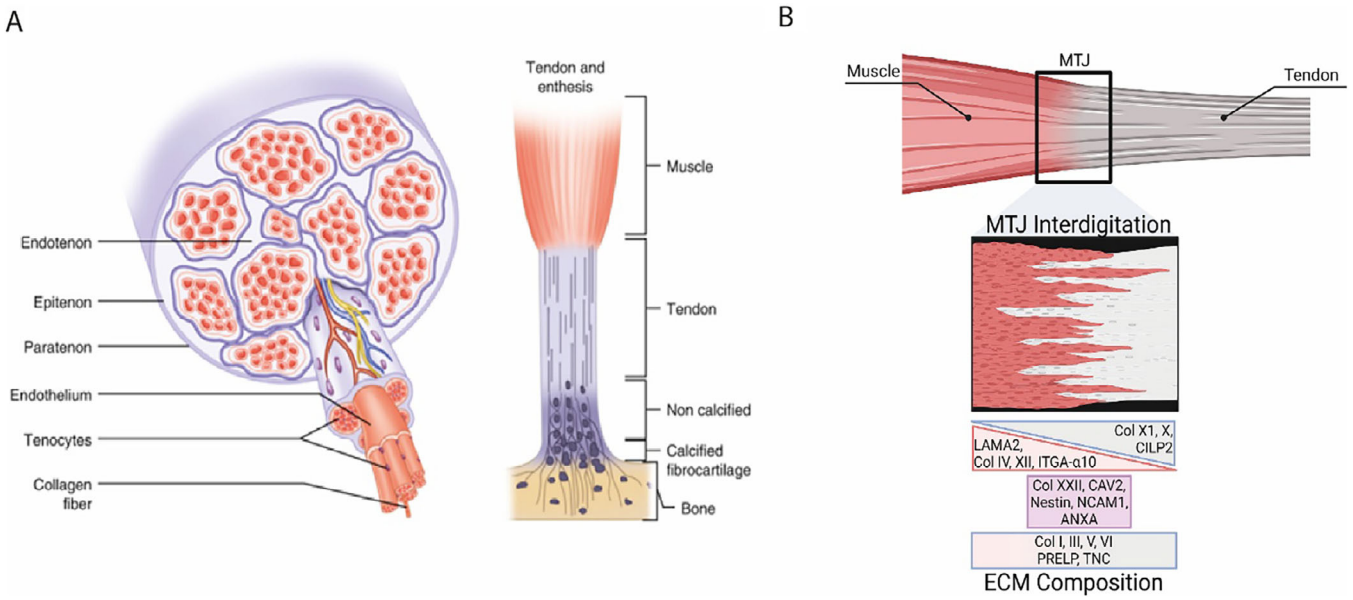

FIGURE 1 (A) Schematic illustration of tendon hierarchical structure and its interface with bone. The left panel depicts the microarchitecture of a tendon, while the right panel illustrates the tendon-to-bone enthesis, emphasizing the transition from muscle to bone through distinct regions: the tendon, noncalcified fibrocartilage, and calcified fibrocartilage. Reproduced with permission from Winters et al.[15] (Copyright 2019). (B) Schematic representation of the myotendinous junction (MTJ), showing the structural transition from muscle to tendon. The illustration highlights ECM composition and the interdigitated architecture, essential for mechanical stability and force transmission. Reproduced with permission from Shama et al.[13]

vascular repair in both muscle and T. Adipocytes, found in healthy MTJs, likely affect remodeling through cytokine signaling.

The whole T/Ls hierarchical architecture contributes to their significant mechanical resistance. The outermost layer of this architecture, the paratenon (Figure 1), is composed of an elastic loose connective tissue allowing the T's smooth gliding against surrounding tissues.

Contiguously, the underlying epitenon is composed of a network of type I collagen fibers that work as a secondary gliding interface.[16] The epitenon is intimately connected with the endotenon, a loose connective tissue collecting single T fibers into fascicles of various sizes. Importantly, the endotenon also has a functional role, since it hosts vascular, lymphatics, and nervous components.[17] Unfortunately, the amount of those components in endotenon is constitutively low, limiting oxygen and nutrients diffusion, ultimately making T/Ls bradytrophic (slow healing)[18–20] tissues.

Collagen is broadly classified into different types based on its structural and functional properties, including fibrillar collagens, fibril-associated collagens with interrupted triple helices (FACITs), and beaded filament-forming collagens.[21] In T/Ls, collagen exhibits a well-defined hierarchical organization, where individual collagen molecules assemble into fibrils, which further aggregate into fibers (primary bundles) and fascicles (secondary bundles).[22]

The ECM of T/Ls is predominantly composed of type I (Figure 2) and type III fibrillar collagen, with a constitutive type I/III ratio (I/III ratio) varying between 1.9 and 4.0, as type I collagen represents the 65–80% of T/L dry weight.[23] T/Ls injuries induce a transient inversion of I/III ratio that spontaneously normalizes during the healing process, making this value a reliable marker for the T/Ls injury recovery.[24]

The T/L's ECM contains lower amounts of different collagen chains such as type V, VI, XII, and XIV collagen.[5] Type V collagen is localized at the core of type I collagen fibrils, playing a role in fibrillogenesis and regulating fibril size. FACIT collagens, such as types XII and XIV, serve as molecular bridges between type I collagen and other matrix components. Furthermore, type XII stabilizes collagen fibers, while type XIV regulates fibril diameter. Type VI collagen, abundant in pericellular regions, forms various polymeric structures: beaded microfilaments, broad-banded structures, and hexagonal lattices. Its absence disrupts fibril organization, leading to a reduction in cross-sectional area.[26]

Besides collagen, non/collagenic molecules complete the T/L ECM composition. Elastin is a fibrillar glycoprotein (GP) that is among the most representative noncollagenic molecules in T/Ls since it contributes to 1–2% of the T/L's dry mass. Elastin provides the characteristic elastic behavior to T/Ls, allowing for the re-establishment of

2688268x, 0, Downloaded from https://onlinelibrary.wiley.com/doi/10.1002/VIW.20250063 by CochraneItalia, Wiley Online Library on [16/10/2025]. See the Terms and Conditions (https://onlinelibrary.wiley.com/terms-and-conditions) on Wiley Online Library for rules of use; OA articles are governed by the applicable Creative Commons License

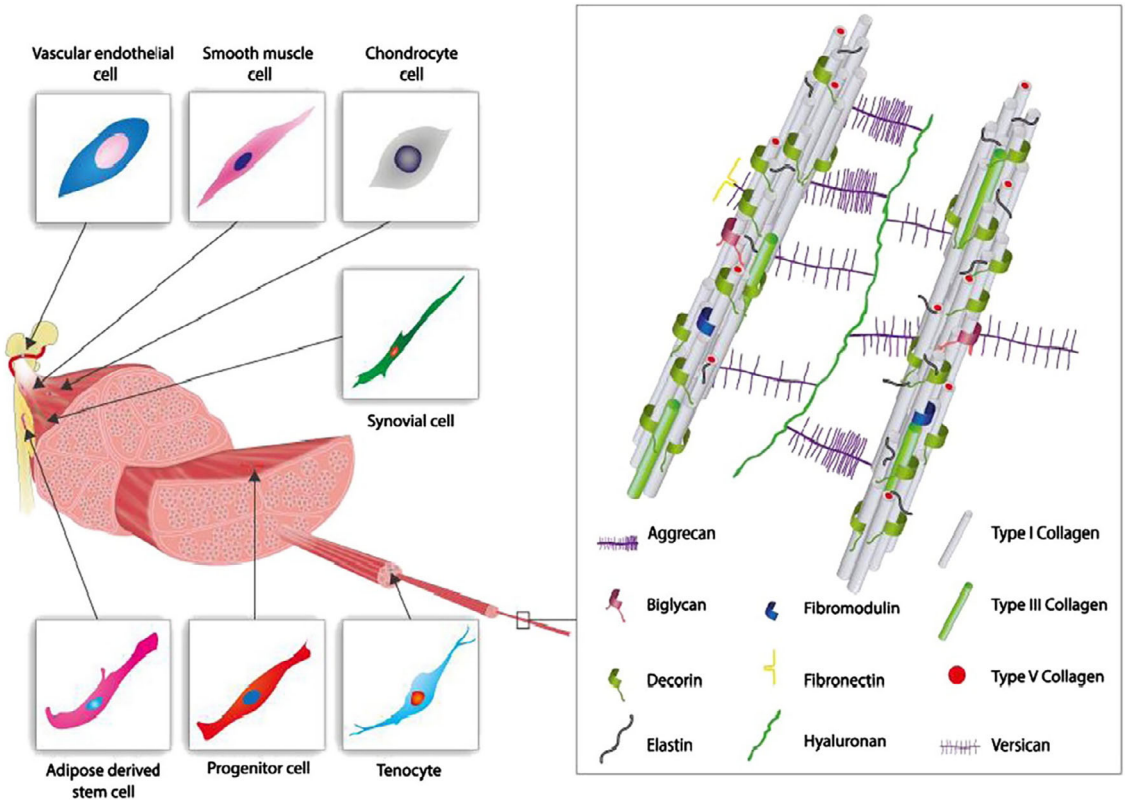

FIGURE 2 Distribution of cells and matrix components within tendons. Reproduced with permission from Lomas et al.[25]

the T/L's native coil architecture after cyclical mechanical deformations.[27,28] The remaining T/L's ECM is composed of different biomolecules such as glycosaminoglycans (GAGs), proteoglycans (PGs), and GPs (Figure 2), which provide a structural integrity to the ECM filling the intrafibrillar space, ultimately resulting in the characteristic T/L's viscoelastic properties. GAGs, such as dermatan sulfate, chondroitin sulfate (CS), heparan sulfate, keratan sulfate, and the nonsulfated hyaluronic acid (HA), are highly hydrophilic molecules that regulate tissue hydration. This property influences both fiber organization and tissue's resistance to transversal compression, contributing to the overall mechanical behavior of T/Ls. Among PGs, decorin (DCN) and biglycan (BGN) are the most representative playing a structural role in maintaining the T/L's fibers architecture. Interestingly, the expression of DCN and BGN genes related are increased during the early stages of T regeneration and remodeling phase[25], respectively, suggesting for an involvement of these PGs in the T/L's self-healing phenomena. Tenomodulin (TNMD) is one of the most abundant transmembrane GPs in T/Ls and is involved in collagen fibril maturation. Tenascin-C (TNC) is another important GPs as its production increases under mechanical load, ultimately regulating the collagen fibers alignment.

1.1.2 | Cells

Mature T/Ls are characterized by low density[29] cell population composed of 90% of tenoblasts and tenocytes. Tenoblasts are undifferentiated cells histologically characterized by a round shape and a large oval nucleus. They are located in the endotenon and remain in their undifferentiated phenotype until their terminal differentiation toward adult tenocytes during the T/Ls maturation. Tenocytes are characterized by a fibroblast-like morphology showing an elongated cell body and a thin cytoplasm[24] (Figure 2). Notably, these cells show a characteristic arrangement that follows a parallel disposition with collagen fibers in ECM, ultimately resulting in an aligned spatial disposition.

The remaining 10% of T/Ls cell compartment is composed of a heterogeneous population, including, synovial cells, chondrocytes (CHs), vascular cells, smooth muscle cells, and T stem/progenitor cells (TSPCs).[17] Interestingly, two different TSPCs sub phenotypes (type I and II)[17] have been identified so far, which are regionally distributed in the epitenon and endotenon, respectively.[29] Remarkably, epitenon-derived TSPCs-I exhibit high levels of vascular- and pericyte-specific markers, whereas endotenon-derived TSPCs (TSPCs-II) are characterized by higher proliferation rates and higher levels of T differentiation-related

2688268x, 0, Downloaded from https://onlinelibrary.wiley.com/doi/10.1002/VIW.20250063 by CochraneItalia, Wiley Online Library on [16/10/2025]. See the Terms and Conditions (https://onlinelibrary.wiley.com/terms-and-conditions) on Wiley Online Library for rules of use; OA articles are governed by the applicable Creative Commons License

markers, compared with TSPCs-I[30], suggesting for two slightly different stages in the TSPCs differentiation path.

Intuitively, scientists should be aware of such a dynamic TSPCs-I/II equilibrium and adopt high-standards handling procedures during experimental manipulation to avoid unwanted phenotype switching and consequential unreliable results. Similarly, a phenotype modification has been noticed for mature tenocytes, making the engineering of T/Ls a challenging task.[20] These cells easily suffer trans-differentiations toward chondrogenic, osteogenic, myogenic, or even adipogenic phenotypes, since they share mesenchymal stem cells (MSCs) as a common biological precursor.[28,31,32] Luckily, this phenomenon can be easily controlled by assessing the expression of tenocyte-specific markers during the tenocytes handling. Obviously, the optimal experimental setup should maximize the expression of positive markers (e.g., COLI, COLIII, SCX, TNMD), minimizing at the same time the expression of negative markers such as COLII (cartilage-associated collagen), alkaline phosphatase ALP (an enzyme involved in the bone mineralization), RUNX2 (activates and regulates osteogenesis), and SOX9 (a transcription factor that participates in sequential events in chondrogenesis).[33] With this aim, several parameters have been found to avoid cell trans-differentiation such as the O_2 tension, the relative concentration of micro/macronutrients in culture media, the presence of specific growth factors, and the substrate topography.[28,34]

1.2 | Mechanical properties

The orientation of collagen fibrils is primarily responsible for the T/Ls high mechanical resistance and viscoelastic behavior, which are both dependent on the magnitude of the applied stress and on the stress application rate. The viscoelastic nature of T/Ls at lower strain rates makes those tissues highly deformable and capable of absorbing a great amount of mechanical energy.[35] Conversely, at high strain rates, T/Ls become stiffer and more proficient in transmitting significant muscle-to-bone and bone-to-bone forces.[36]

Water content is a key modulator of T/L biomechanics at both macro and micro scales. Notably, elastic modulus and tensile strength increase significantly with decreasing water content, while strain at failure remains unaffected.[37] The T/Ls biomechanics have been established by creating stress–strain curves using different mechanical tests.[4] Regardless of the test adopted, the overall stress–strain curve exhibits a nonlinear behavior composed of four distinct regions.[38] When the tissue is stretched, the energy is involved in the system's entropy reduction; therefore, the mechanical stress does not induce any tension response in the tissue. This behavior is described by the first part of the stress–strain graph, where a low slope of the nonlinear portion (toe region) (Figure 3) and a gradual slope increase are visible until the first part of the linear zone. In the toe region of the stress–strain curve, collagen crimps are gradually straightened, leading to a nonlinear response. In Ts, this toe region is relatively short (until 2%) and consistent across the body. In contrast, Ls, which accommodate varying joint motions, display more variable toe regions depending on their anatomical location.[39] As the fibers align, stiffness increases and the curve transitions into the linear region. Specifically, the T/Ls mechanical behavior exhibits a linear stress–strain response for deformations between 2 and 6%, characterized by an elastic modulus ranging from 0.5 to 2 GPa (Table 1). At this stage, deformations are reversible as the tissue returns to its initial length when the load is removed. Deformations exceeding 6% induce an interfiber crosslink breaking-up, allowing fibers to slide over adjacent fibers and triggering a plastic deformation (microscopic breakage). The slope of the curve decreases due to intense tissue damage (macroscopic breakage) that continues until a complete failure, which is typically reached at deformations greater than 8%.[38]

Intuitively, the mechanical behavior varies greatly depending on the anatomical region where T/Ls are inserted to. As an example, muscles responsible for precise movements (e.g., the flexors of the fingers) rely on thin Ts, while muscles requiring high levels of strength and endurance (e.g., quadriceps and triceps surae) are connected to bone via larger Ts.

Another mechanical property of interest is the Poisson's ratio, which quantifies the ratio of lateral strain to longitudinal strain during uniaxial deformation.[54] Although commonly assumed to be positive, some materials, including biological tissues like skin, and arteries exhibit a negative Poisson's ratio (auxetic behavior), meaning they expand laterally when stretched longitudinally. Recent in vivo and ex vivo investigations have revealed that healthy human and animal Ts display auxetic characteristics, thus offering new insights on their mechanical behavior.[55]

A plethora of studies focused on T/Ls mechanical properties at various size scales have been extensively conducted.[27] The wide range of reported mechanical properties in human T/Ls reflects the technical challenges of characterizing these tissues ex vivo.[56] Factors such as precise dissection and clamping, accurate measurement of T's dimensions (including cross-sectional area), and the need for theoretical models to interpret biological material properties all contribute to this variability. As a result, a single definitive value for a given T cannot be determined. Consequently, in vivo measurements relying on noninvasive assessment of human T/Ls lengthening during voluntary muscle contraction serve as a benchmark.

2688268x, 0, Downloaded from https://onlinelibrary.wiley.com/doi/10.1002/VIW.20250063 by CochraneItalia, Wiley Online Library on [16/10/2025]. See the Terms and Conditions (https://onlinelibrary.wiley.com/terms-and-conditions) on Wiley Online Library for rules of use; OA articles are governed by the applicable Creative Commons License

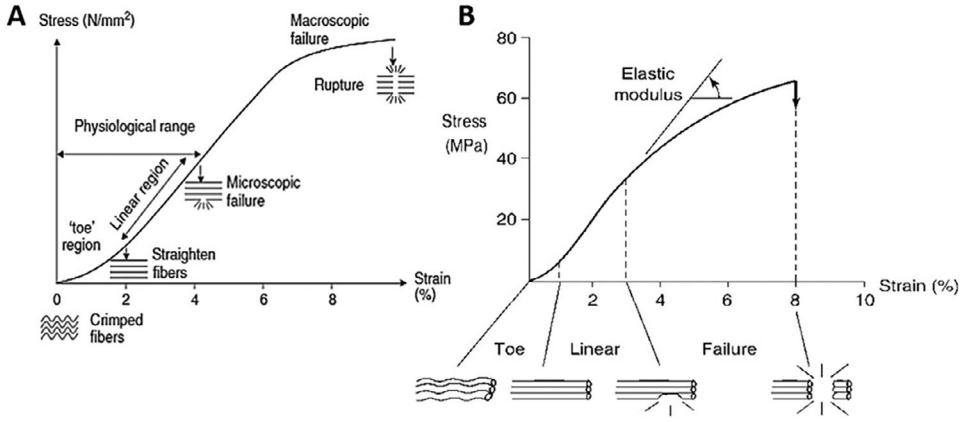

FIGURE 3 Typical response of tendon tissues. This graph illustrates the stress–strain curve of tendons, demonstrating their biomechanical properties across different phases of deformation. The top section visually represents collagen fiber morphology during stretching: (1) crimped fibers at rest, (2) straightened fibers under load, (3) microfailure, and (4) complete rupture. Reproduced with permission from Rinoldi et al.[40]

TABLE 1 Mechanical properties of human T/L tissues.

Sorted tendon	Functional test	Elastic modulus (MPa)	Maximum load (N)	Maximum stress (MPa)	Maximum strain (%)	References
Achilles tendon	Ex vivo	819 ± 208	5098 ± 1199	79 ± 22	8.8 ± 2.2	41
Gastrocnemius tendon	In vivo	1160 ± 150	875 ± 85	32.4 ± 2.3	4.9 ± 1%	42
Patellar tendon	In vivo	597.4 ± 48.5	5452.7 ± 307.3	48 ± 2	4.86 ± 0.5	43
Achilles tendon	In vivo	1900 ± 500	1924 ± 229	29 ± 3	4.2 ± 1.1	44
Achilles tendon	In vivo	870 ± 200	~5000	~75	8.3 ± 2.1	45
Tibialis anterior tendon	In vivo	1200 ± 150	530 ± 59	25 ± 2.5	2.5 ± 0.4	46
Extensor hallucis longus tendon	Ex vivo	448 ± 183	316 ± 88	39 ± 18	11.7	46
Tibialis posterior tendon	Ex vivo	187 ± 54	475 ± 60	19 ± 5	16.3	47
Flexor hallucis longus tendon	Ex vivo	440 ± 119	525 ± 200	26 ± 10	12.3	47
Long head of the biceps tendon	Ex vivo	282.9 ± 144	–	31.7 ± 15.4	11.6 ± 6.6	48
Posterior cruciate ligament	Ex vivo	248 ± 119	1620 ± 500	35.9 ± 15.2	18 ± 5.3	49
Anterior cruciate ligament	Ex vivo	128 ± 35	1818 ± 699	26.35 ± 10.8	30 ± 6	50
Periodontal ligament	Ex vivo	4.50 ± 1.01	–	0.4	0.103	51
Femural arcuate ligament	Ex vivo	–	78.2 ± 37.9	6.61 ± 3.52	15 ± 7.5	52
Tibionavicular ligament	Ex vivo	320.7 ± 268.5	120 ± 49	22.93 ± 16.82	10 ± 2	53
Posterior tibiotalar ligament	Ex vivo	99.54 ± 79.32	467 ± 209	15.99 ± 15.07	30 ± 13	53

2688268x, 0, Downloaded from https://onlinelibrary.wiley.com/doi/10.1002/VIW.20250063 by CochraneItalia, Wiley Online Library on [16/10/2025]. See the Terms and Conditions (https://onlinelibrary.wiley.com/terms-and-conditions) on Wiley Online Library for rules of use; OA articles are governed by the applicable Creative Commons License

In this context, new experimental approaches for measuring deformation and strain have been introduced to overcome the limitations of classical mechanical testing. Among these, digital image correlation (DIC) has gained attention as a noninvasive optical technique for full-field strain analysis.[57] By tracking a random speckle pattern on the specimen's surface, DIC allows high-resolution and sub-pixel measurements of displacement.[58] When combined with stereo camera systems, it enables three-dimensional mapping of strain magnitude and distribution across the tissue.[59] Despite its promising potential, applications of DIC to T/Ls remain limited in the literature.[58]

A summary of the key mechanical properties of various human T/Ls is provided in Table 1.

1.3 | T/L injuries , healing process, and therapeutic approaches

T/Ls disorders may be categorized into two macro-groups (acute, and chronic disorders) that overall describe the diseases' onset time. Specifically, acute injuries occur after sudden traumas following intense physical stresses due to agonistic sport activities, or undesirable nonphysiological movements. Chronic injuries are consequential of untreated/mistreated injuries instead and often hit elderly people suffering from recurrent mechanical breakdowns and related inflammatory processes. Both acute and chronic T/Ls disorders cause well-defined pathological conditions described as tendinopathy, tendinitis, and tendinosis, but their etiology and physiopathology are often foggy and confusing.

Tendinopathy is typically used to describe a disorder involving a T without knowing the specific pathology, ultimately leading to severe dysfunctionality and localized pain. It is primarily diagnosed through anamnestic investigation supported by semeiotic examination. Despite the involvement of massive phlogistic phenomena, recent findings classify tendinopathies as degenerative processes triggered by a defective self-healing response.[60] Tendinitis refers to a TI accompanied by an inflammatory response and the presence of inflammatory cells caused by an overloading of the musculotendinous unit.[61] In contrast, tendinosis describes the noninflammatory degeneration of a T, as identified histopathologically,[60] which can include changes to its structure or composition.

The healing process following TI occurs in three overlapping stages: inflammation, proliferation, and remodeling. The expression profile of cytokines varies throughout T healing, with proinflammatory cytokines predominating in early phases, while anti-inflammatory and reparative cytokines become more prominent in later stages.[62]

The inflammatory phase begins immediately after the injury with a clot formation at the damaged site and lasts approximately 1 week. Platelets and cells within the clot release key factors, including transforming growth factor-β (TGF-β), insulin-like growth factor-1 (IGF1), and platelet-derived growth factor (PDGF). These factors help establish a local environment that supports the recruitment of inflammatory cells, such as interleukins (IL), IL-6 and IL-1β.

Growth factors recruit neutrophils from the bloodstream, which in turn activate M1 macrophages to clear necrotic debris through phagocytosis. Simultaneously, cytokine-recruited fibroblasts migrate to the injury site and initiate matrix deposition, marking the beginning of the healing process.

The proliferative phase begins approximately 2 days postinjury and is characterized by ECM expansion, fibrous scar formation, and increased cell activity. During this phase, TGF-β levels peak, and macrophages gradually shift to M2 phenotype, which later contributes to scar remodeling. TGF-β drives collagen production, recruits TSPCs, and regulates protease activity, whereas IGF promotes ECM production. PDGF is involved in DNA and protein synthesis. As healing progresses, TSPCs proliferate and differentiate into tenocytes which, along with fibroblasts, contribute to tissue regeneration by depositing PGs, GAGs, and collagen at the wound site.

The remodeling phase begins 2 weeks following the injury and is marked by the reorganization of previously synthesized collagen. The whole phase is characterized by a gradual decrease in cellularity alongside an increase in collagen content and density. Tenocytes and collagen fibers align longitudinally to enhance the mechanical strength of the newly forming tissue. Collagenase activity promotes the transition from type III to type I collagen, the latter characterized by larger fiber diameter and higher tensile strength. Moreover, tenocytes express α-smooth muscle actin, fundamental in matrix contraction, supporting wound closure. Throughout this phase, tenocytes metabolic activity remains significantly lower compared with the early stages of healing. The overall duration of T repair depends on the severity of the injury and the specific T affected.

Regardless the kind of T/Ls disorder, the inadequate self-healing remains a common challenge, often resulting in the formation of fibrous T/L-like tissue that lacks the native biochemical and biomechanical properties of healthy tissue.[1,63]

The treatment of acute and chronic T/Ls injuries relies on conservative methods, surgical intervention, or a combination of both. Conservative approaches refer to nonsurgical strategies that typically include rest, physiotherapy, cryotherapy, ultrasound therapy, and laser therapy.

2688268x, 0, Downloaded from https://onlinelibrary.wiley.com/doi/10.1002/VIW.20250063 by CochraneItalia, Wiley Online Library on [16/10/2025]. See the Terms and Conditions (https://onlinelibrary.wiley.com/terms-and-conditions) on Wiley Online Library for rules of use; OA articles are governed by the applicable Creative Commons License

Additionally, pharmacological therapies often involving nonsteroidal anti-inflammatory drugs and corticosteroids are commonly employed to manage pain and inflammation.[64] However, the inherently limited self-healing capacity of T/Ls frequently reduces the effectiveness of conservative treatments, often leading to partial functional loss and recurrent injuries.[65]

A key factor in determining the appropriate treatment strategy is the severity of the injury. Massive injuries like ruptures typically require surgical intervention, while chronic injuries, if left untreated, can lead to progressive T weakening, muscle atrophy, contractures, and reduced joint mobility.[66]

Although conservative treatment can help avoid the complications of surgery such as infections, scar formation, T necrosis, nerve damage, and the risk of retears, surgical intervention remains the primary approach for the treatment of severe injuries.[2] Conventional surgical techniques focus on restoring the biomechanical properties of the T through wound suturing or securing the T to the bone using sutures, wire loops, and stainless-steel anchors. Both open-air and arthroscopic repair techniques are widely employed, often in combination with postoperative conservative rehabilitation to accelerate functional recovery (known as combined approach). However, while surgery can temporarily restore T continuity, it does not fully preserve the structural integrity, resulting in a retear risk ranging from 26% for small (<1 cm) and medium (1–3 cm) tears to 94% for large (3–5 cm) and massive (>5 cm) tears[63]

Tissue grafting is an alternative surgical approach in which a T graft is used to bridge the damaged area.[67] Autografts, derived from an autogenous donor T, are preferred to minimize the risk of immune rejection but they come with potential complications, including donor site morbidity, and only partial restoration of T/L pre-injury functionality (approximately 50%).[67] Allografts (from one individual and transplanted into another individual) and xenografts (from nonhuman species) serve as alternatives when the autografts are unavailable, such as multi-LIs or revision surgeries. However, they carry their own set of risks including tissue rejection and disease transmission,[5,62] often requiring lifelong immunosuppressive therapy to prevent graft rejection. Moreover, tissue grafting approaches are often less effective in chronic injuries, as they can lead to excessive postoperative tension, with failure rates reaching up to 38%.[2]

In the current medical landscape, it is important to recognize that although conservative approaches, traditional surgery, and the use of grafts have played a fundamental role, they have inevitable intrinsic limitations that are prompting an increasing interest in TE as a promising and innovative perspective.

The term "tissue engineering" was first introduced by participants at the first meeting sponsored by the National Science Foundation in 1988 even though at that time it had a poor connection to the discipline as it is conceived today.[68] In 1993, Langer and Vacanti summarized the early developments in this field by defining TE as "an interdisciplinary field that applies the principles of engineering and the life sciences toward the development of biological substitutes that restore, maintain, or improve tissue function."[69]

TE often begins with cell in vitro expansion under controlled conditions to promote their growth and proliferation. Then, these cells are seeded onto a biocompatible matrix or *scaffold*—a structural framework made of synthetic or natural materials that support tissue growth before implantation. Over time, the biodegradable biomaterial undergoes gradual degradation within the body, while the implanted cells proliferate and secrete ECM in vivo, ultimately leading to the repair of damaged tissue. For scaffolds to be effective and minimize side effects, they must meet several criteria, such as nontoxic degradation products, biocompatibility, a degradation rate that matches tissue growth, adequate porosity, and mechanical strength.

2 | THE ROLE OF BIOMATERIALS IN SCAFFOLDS DESIGN

One of the main design principles in TE is biomimicry, which is the ability to replicate the native biological environment of the tissue. From a biomimetic perspective, a scaffold designed for T/L TE should ideally exhibit anisotropic mechanical properties, mimicking the natural alignment of collagen fibers[16] that respond differently depending on the direction of the applied force.[70] Additionally, scaffolds should possess a hierarchical structure, reflecting the multiscale organization of T/Ls, which spans from a molecular to a macroscopic level.

Despite the many advantages provided by metallic and ceramic materials, polymers are particularly well suited for scaffolds biofabrication, thanks to their biocompatibility and processability.[71] The choice between natural and synthetic polymers depends on the specific application.

2.1 | Natural polymers

Natural polymers, such as collagen, chitosan, silk, or HA, offer low immunogenicity and a biological environment that supports cell adhesion and growth, exhibiting minimal immunogenicity. As intrinsically bioactive, they have been extensively explored in T/L TE. Moreover, different strategies have been employed to

2688268x, 0, Downloaded from https://onlinelibrary.wiley.com/doi/10.1002/VIW.20250063 by CochraneItalia, Wiley Online Library on [16/10/2025]. See the Terms and Conditions (https://onlinelibrary.wiley.com/terms-and-conditions) on Wiley Online Library for rules of use; OA articles are governed by the applicable Creative Commons License

overcome their inherent limitations, particularly in terms of mechanical performance and degradation control. One notable approach was proposed by Tawonsawatruk and colleagues,[72] who leveraged the hyperplastic polymer polyhydroxyalkanoate, produced by microorganisms like *Pseudomonas,* to fabricate T/L implants. By threading human plantaris through molds with predesigned holes, they created a composite graft with a tensile strength of 56 MPa, closely resembling that of a human hand T. Hydrogel-based scaffolds have gained increasing attention due to their ability to support cell functions while replicating the hydrated environment of native tissues. For example, Diaz and colleagues[73] developed a scaffold for supraspinatus T repair using a chitosan–gelatin matrix with varying cellulose concentrations. Crosslinking with genipin improved the scaffold's stability, while cellulose incorporation enhanced cell metabolic activity and proliferation. A different strategy was explored by Ruiz-Alonso and coworkers[74] who engineered a hydrogel-based scaffold composed of alginate, HA, gelatin, and fibrinogen. This formulation exhibited remarkable biocompatibility, facilitating tenocytes recovery from bioprinting-induced stress and promoting rapid cell proliferation, while preserving their phenotype. Further advancing hydrogel-based strategies, Li and colleagues[75] proposed a 3D hydrogel-based sandwich model in which TSPCs were cultured on a grooved 2D hydrogel substrate before an additional hydrogel layer was added to form a 3D construct. In vivo implantation in a rat Achilles T defect model demonstrated not only enhanced T regeneration but also a reduction in heterotopic ossification.

Despite these promising advantages, natural polymers still pose significant challenges, including uncontrolled degradation rates and mechanical properties that do not fully match those of Ts.[63] Moreover, batch-to-batch variability in molecular weight and purity can compromise reproducibility, thereby limiting their clinical applicability.

2.2 | Synthetic polymers

Unlike natural polymers, synthetic polymers such as poly(lactic-co-glycolic acid) (PLGA), polylactide (PLA), polycaprolactone (PCL), and polyurethane (PU) offer superior mechanical properties and tunable degradation rates. They enable precise control over scaffold architecture, porosity, and degradation kinetics. Moreover, synthetic polymers can be engineered to meet the mechanical properties of native T tissue, providing temporary support during healing.[76] One approach to improving the bioactivity of synthetic scaffolds was demonstrated by Wang's team, who developed a PLGA scaffold functionalized with PDGF-AA (PLGA–PDGF-AA) onto the surface of PLGA fibers. Functionalization significantly enhanced T repair, as in vitro experiments confirmed the scaffold's biocompatibility and lack of cytotoxic effects. In a mouse hind limb TI model, PLGA–PDGF-AA scaffold significantly improved T repair and collagen synthesis compared with PLGA alone. Beyond biochemical modifications, mechanical stimulation has also been explored as a key factor in optimizing synthetic scaffolds for T repair. Wang and colleagues[77] demonstrated that mechanical loading on a cell-free polymeric composite scaffold significantly enhanced the regeneration of a fully functional Achilles T in a rabbit model. The scaffold, composed of a combination of PGA and PLA filament fibers, promoted host cell infiltration, matrix production, and tissue remodeling. Histological analysis showed the formation of parallel-aligned collagen fibers and tenocytes similar to those on native Ts. A different strategy was pursued by Bahrami and colleagues,[78] who used PU to create multiscale nanofibrous scaffolds designed to replicate the architecture and mechanical characteristics of T/Ls fascicles. The bundles closely replicated the mechanical properties of other PU-based grafts, such as Artelon (SportMesh), as well as native T tissues like patellar T. The work by Turgut and coworkers[79] explored the use of fibroblast growth factor-2 (FGF-2) PCL/PU nanofibrous scaffold. In vivo results on rat Achilles TI model demonstrated that the use of FGF-2 effectively supported T healing with a better collagen fibril organization, enhanced vascularity, and reduced inflammatory responses.

Challenges related to biocompatibility, inflammatory responses, and the potential cytotoxicity of degradation byproducts remain significant obstacles in the clinical translation of synthetic polymers. The breakdown of polymeric chains into acidic byproducts can lead to pH changes, subsequently triggering inflammatory reactions.[80] To address these limitations, researchers are actively investigating strategies to improve the biological performance of synthetic scaffolds. For instance, surface modifications such as plasma treatment, bioactive molecule coatings, and functionalization with anti-inflammatory agents have shown promise in reducing immune responses and promoting cell interactions.[81] Furthermore, hybrid approaches combining synthetic polymers with natural polymers, such as collagen or gelatin, can leverage the mechanical advantages of synthetic scaffolds while minimizing adverse reactions.[82]

3 | OPTIMIZING BIOPHYSICAL AND STRUCTURAL CUES

T/Ls are mechanosensitive tissues that experience continuous mechanical stretching, a process essential to the

2688268x, 0, Downloaded from https://onlinelibrary.wiley.com/doi/10.1002/VIW.20250063 by CochraneItalia, Wiley Online Library on [16/10/2025]. See the Terms and Conditions (https://onlinelibrary.wiley.com/terms-and-conditions) on Wiley Online Library for rules of use; OA articles are governed by the applicable Creative Commons License

maintenance of T/L cell morphology and phenotype.[83] Besides promoting tenogenic differentiation of stem cells by augmentation of T-specific markers, mechanical loading improves the mechanical properties of the engineered tissues through ECM remodeling and regulation of cell behavior.

A strategy of replicating this native mechanical milieu is the application of mechanical stretching, which can be classified as static and dynamic. Among these types, dynamic stretching is the most employed, whose outcome influenced by three parameters: strain, frequency, and rest intervals. Each of these factors independently impacts tenogenic differentiation, thus their interdependence complicates the determination of optimal conditions. To address this challenge, advanced bioreactors have become essential.[83] Such systems regulate multiple variables simultaneously, thereby closely mimicking the biomechanical and biochemical environment of native T/Ls, which consequently delivers the required stimuli to the engineered constructs. Bioreactors serve multiple purposes, including investigating fundamental biological pathways, engineering tissue substitutes, preserving organ function ex vivo, and conditioning therapeutic cells before transplantation.[84] For instance, Xu and team[85] investigated the effects of mechanical stimulation on TSPCs cultured on poly(L-lactide-co-ε-caprolactone)/collagen scaffolds using a custom-made 3D bioreactor. The results of their research demonstrated that cyclic tensile strain at different frequencies (0.3, 0.5, and 1.0 Hz) and amplitudes (2, 4, and 8%) did not compromise cell viability. However, differences in cell proliferation and T-specific marker expression were observed, and the optimal response was achieved at 0.5 Hz and 4% strain. In a study led by Qiu and coworkers,[86] hMSCs were subjected to cyclic mechanical loading (10% strain, 1 Hz, 3-h on/off cycles for 14 days) significantly upregulated T-related ECM proteins, including COLI, COL III, and TNC. Bosworth and colleagues[87] fabricated PCL electrospun yarns seeded with hMSCs and subjected to dynamic tensile loading. Scaffolds exposed to a sinusoidal tensile loading regimen (5% strain, 1 Hz, 1 h daily) developed a visibly thicker cellular layer on their outer surface compared with those maintained under static conditions. This suggests enhanced cell proliferation and/or ECM production, while preserving a primarily uniaxial alignment of the cells. Similarly, Lee and their team[88] cultured human L fibroblasts on electrospun-aligned PU nanofiber sheets. Results showed that fibroblasts cultured on aligned nanofibers had a similar morphology to L fibroblasts in vivo, as well as enhanced ECM production when exposed to 5% cyclic strain at 0.2 Hz using a modified Flexcell bioreactor.

Apart from mechanical stimuli, scaffolds design is a key player in T/Ls repair, with porosity being one big factor. An optimized pore structure allows the scaffold to function as a cytoskeletal substitute during the initial stages of healing, where cell elongation and migration are promoted. Moreover, deeper pore architectures provide the necessary space for cell proliferation and ECM deposition.

Beyond porosity, the recreation of hierarchical organization of T/L ECM is another fundamental prerequisite in scaffold design. To this end, biomaterials with aligned topographies have been developed, as they resemble the native T/L microenvironment, promoting aligned collagen fiber deposition[89] and tenogenic differentiation.[90]

4 | SCAFFOLD MANUFACTURING TECHNIQUES FOR T/L SCAFFOLDS

The choice of the biofabrication approach greatly influences the properties of the scaffold and is driven by the severity of the injury and the type of T involved.[5]

Several fabrication techniques have emerged as prominent strategies in T/L TE including 3D printing, electrospinning, melt electrowriting (MEW), and decellularization (Figure 4). Each of these techniques possess distinct benefits and drawbacks (Table 2). 3D printing provides accurate control over scaffold geometry, allowing the design of customized architectures tailored to specific functional requirements. Electrospinning enables the production of nanofibrous structures with high porosity and surface area, facilitating cell attachment and proliferation. MEW, a variation of electrospinning, uses a heated polymer to generate well-organized and customizable fiber arrangements. Textile-based fibrous scaffolds offer significant advantages of scalability and versatility, and they can be engineered to mimic the architecture of T/Ls.[20] Decellularization is another widely used technique aimed at removing cell components while preserving the ECM's structural integrity. Moreover, new technologies grouped as "hybrid fabrication techniques" have gained attention for their ability to integrate multiple materials and architectures into a single construct, offering new possibilities for scaffold optimization.

To make easier the comprehension of the Section 4, we included a schematic overview of the different fabrication techniques adopted for T/Ls scaffolds, highlighting their respective advantages and drawbacks (Table 2).

4.1 | 3D printing

3D printing is an additive manufacturing method based on computer-aided design that creates 3D structures in a layer-by-layer fashion starting from a 2D pattern and using a liquid binder that is printed onto a powder bed.

2688268x, 0, Downloaded from https://onlinelibrary.wiley.com/doi/10.1002/VIW.20250063 by CochraneItalia, Wiley Online Library on [16/10/2025]. See the Terms and Conditions (https://onlinelibrary.wiley.com/terms-and-conditions) on Wiley Online Library for rules of use; OA articles are governed by the applicable Creative Commons License

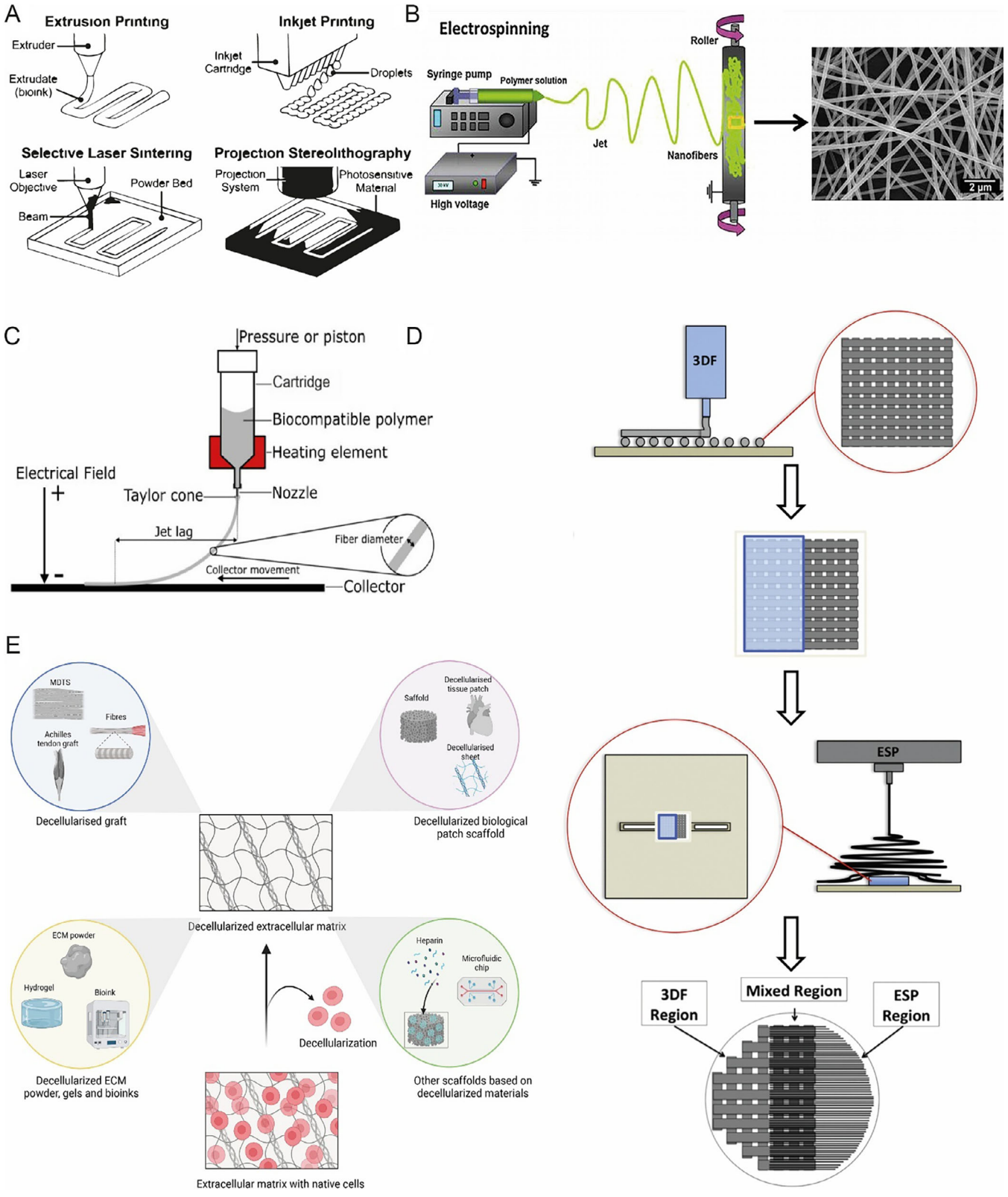

FIGURE 4 Schematic overview of the main fabrication techniques employed for T/L scaffolds. (A) 3D printing including extrusion printing, inkjet printing, selective laser sintering, and projection stereolithography (reproduced with permission from Miller et al.[91]). (B) Electrospinning for the fabrication of nanofibrous meshes (reproduced with permission from Rahmati et al.[92]). (C) Melt electrowriting for the precise deposition of microfibers under an electric field (licensed under CC BY 4.0 from Loewner et al.[93]). (D) Hybrid fabrication strategies (Criscenti et al.[94]). (E) Decellularization techniques for generating ECM-based scaffolds from native tissues (reproduced with permission from Zhong et al.[95]).

26882568x, 0, Downloaded from https://onlinelibrary.wiley.com/doi/10.1002/VIW.20250063 by CochraneItalia, Wiley Online Library on [16/10/2025]. See the Terms and Conditions (https://onlinelibrary.wiley.com/terms-and-conditions) on Wiley Online Library for rules of use; OA articles are governed by the applicable Creative Commons License

TABLE 2 Overview of advantages and disadvantages of the main fabrication techniques employed in T/L TE.

Fabrication technique	Advantages	Disadvantages	Scaffold composition	Experimental model	Implant site	References
3D printing	Rapid prototyping Design freedom	Limited resolution Postprocessing required	GelMa/PCL	In vitro and in vivo (rat)	Achilles tendon	75
			PCL	In vitro	–	96
			PLA	In vitro	–	97
			PLGA/collagen/fibrin	In vitro and in vivo (mouse)	Back subcutaneous implantation	98
			PCL/pluronic F127	In vitro and in vivo (rat)	Achilles tendon	99
Electrospinning	High surface area to volume ratio Submicron dimensions High pores interconnections Tunable properties	Challenges in collecting and handling nanofibers Trapped solvents require removal from electrospun nanofibers Low production yield	PPDO/SF	In vitro and in vivo (rat)	Subcutaneous implant	100
			PLA PLCL/Collagen I	In vitro and in vivo (rabbit) In vitro and in vivo (mouse)	Anterior cruciate ligament Back subcutaneous implantation	101, 102
			PLGA/chitosan/sTECM	In vitro and in vivo (mouse)	Achilles tendon	103
			PCL/gelatin	In vitro and in vivo (rabbit)	Patellar tendon	104
			PDO	In vitro	–	105
			PCL/SF	In vitro and in vivo (rat)	Achilles tendon	106
			PCL/PTMC–MA PCL	In vitro In vitro	– –	107, 108
			PCL	Ex vivo	–	109
	–		PCL/ChS	In vitro and in vivo (rat)	Rotator cuff tendon	110
			PCL	In vitro	–	111

(Continues)

26882568x, 0, Downloaded from https://onlinelibrary.wiley.com/doi/10.1002/VIW.20250063 by Cochraneltalia, Wiley Online Library on [16/10/2025]. See the Terms and Conditions (https://onlinelibrary.wiley.com/terms-and-conditions) on Wiley Online Library for rules of use; OA articles are governed by the applicable Creative Commons License

TABLE 2 (Continued)

Fabrication technique	Advantages	Disadvantages	Scaffold composition	Experimental model	Implant site	References
Melt electrowriting	Highly organized structures Highly controlled pore size and interconnectivity	Careful control of temperature to avoid material degradation Low production speed	PCL/collagen I	In vitro		112
			p(e-CL-AC)	In vitro	–	113
Electrospinning/textile technologies	High surface area Fabrication of complex structures Enhanced mechanical properties	Production costs Limited scalability Need for specialized expertise	PLLA/SF	In vitro and in vivo (rat)	Achilles tendon	114
			PLGA	In vitro and in vivo (rat)	Achilles tendon	115
			PCL	In vitro and in vivo (rabbit)	Extensor digitorum tendon	116
3D printing/ electrospinning	Structural customization Enhanced mechanical properties	Production costs Time-consuming fabrication	PLA/PCL/gelatin	In vitro and in vivo (rat)		117
			PLGA/PCL	In vitro	–	94
			PDO/PCL	In vitro	–	118
			PCL/PLGA	In vitro	–	119
Decellularization	Biocompatibility Preformed structure	Inferior mechanical properties Low reproducibility Complex process	ECM from rat Achilles tendon	In vitro	–	120
			ECM from bovine Achilles tendon	In vitro and in vivo (rat)	Achilles tendon	121
			ECM from mussel adductor muscle	In vitro and in vivo (rat)	Achilles tendon	122
			ECM from pig connective tissue	In vitro and vivo (human)	Supraspinatus tendon	123

Abbreviations: GelMA, gelatin methacrylate; PCL, polycaprolactone; PLA, poly(lactic acid); PLGA, poly(lactic-co-glycolic acid); PPDO, poly(p-dioxanone); SF, silk fibroin; PLCL, poly(L-lactide-co-ε-caprolactone); sTECM, soluble tendon extracellular matrix; PDO, polydioxanone; PTMC–MA, methacrylated poly(trimethylene carbonate); ChS, chitosan; p(e-CL-AC), poly(e-caprolactone-co-acryloyl carbonate); PLLA, poly (L-lactic acid); ECM, extracellular matrix.

26882568x, 0, Downloaded from https://onlinelibrary.wiley.com/doi/10.1002/VIW.20250063 by Cochraneltalia, Wiley Online Library on [16/10/2025]. See the Terms and Conditions (https://onlinelibrary.wiley.com/terms-and-conditions) on Wiley Online Library for rules of use; OA articles are governed by the applicable Creative Commons License

The technique is characterized by a precise control over biomaterial deposition at the micrometer level, with the possibility to achieve controllable porosity (both in geometry and size) and an accurate replication of the macroscopic architecture of native tissues.[124] Through 3D printing, multiple materials can be combined in the same scaffold, with a broad design space, ranging from plain structures (like patches, or sheaths)[96–98,104,125] to more complex tubular shapes[99,101,116]

Different 3D printing techniques have been developed, including stereolithography, bioprinting, inkjet printing, fused deposition modeling (FDM), selective laser sintering, and laser beam melting.[91] While each has its technical realization, the common principle among them is the sequential addition of material in a layer-by-layer manner to achieve the final structure.[124] Current research has demonstrated the application of 3D printing for T regeneration through the utilization of different combinations of materials.

Li and colleagues[75] fabricated a gelatin methacrylate (GelMa)/PCL scaffold. In the study, the PCL shell was used to enhance the mechanical properties of the hydrogel core. Functional assessments in a rat Achilles T defect model showed that the scaffold can promote T regeneration while preventing heterotopic ossification. Similarly, Kempfert and colleagues[96] developed a PCL patch coated with collagen I and fibronectin to increase the overall biocompatibility. Additionally, authors performed plasma modifications that further enhanced the hydrophilicity of the construct, as showed by experiments with human bone marrow stem cells (BMSCs). Innovative structural designs have also been explored. Rodriguez-Reinoso and coworkers[97] explored a PLA-based device composed of two superposed thin patches featuring barbs inspired by rose thorns and limpet teeth. Their findings indicate that the device provides superior load distribution compared with conventional suture-based methods. Jiang and team[98] enhanced stem cell function and proliferation by incorporating collagen I and fibrin hydrogels into a PLGA scaffolds (Figure 5). In vivo, subcutaneous implantation in mice revealed excellent biocompatibility and degradation properties. Likewise, Zhang and colleagues[99] employed electrohydrodynamic 3D printing to fabricate a PCL scaffold, incorporating Pluronic F127 at different concentrations. In vitro tests showed that PCL scaffolds with 5% F127 exhibited optimal cell adhesion and growth, whereas in vivo data obtained from rats' Achilles demonstrated enhanced collagen deposition and organization.

While there has been enormous advancement in 3D printing, there are still some problems. Among the primary limitations is achieving native T/L biomechanical strength, which requires oriented fibers that mimic natural collagen fibers. However, obtaining aligned fibers with 3D printing technology is challenging. While electrospinning excels in producing aligned nanoscale fibers, conventional 3D printing methods struggle to achieve the same level of organization. Postprinting processes may offer a potential solution to improve scaffold mechanical properties. Moreover, the issue of reproducibility is a significant concern, especially for clinical application. However, ongoing optimization of printing parameters and material selection has already shown promise in improving consistency, suggesting that these limitations may be progressively overcome.

4.2 | Electrospinning

Electrospinning is acknowledged as a versatile technique in used materials science and biomedical engineering which involves the creation of ultrafine fibers through the application of an electric field to a polymer solution. The standard experimental setup for electrospinning relies on a syringe, a spinneret (usually a needle), a syringe pump, a high-voltage power supply, and a collector, which can either be planar or rotary.[126] During the process, the polymeric solution is extruded from the syringe, forming a droplet at the needle tip. Upon application of a high voltage, the droplet elongates into a conical shape known as the "Taylor cone," and a thin liquid jet emerges once the electrical field overcomes the solution's surface tension. As the jet travels toward the collector, it undergoes rapid whipping motion, during which solvent evaporation occurs, leading to fiber deposition. The resulting fibers possess unique properties such as high surface area-to-volume ratio, tunable diameters, flexibility in surface functionalization, and interconnected porous structure.[92] Beyond its material flexibility, electrospinning offers a wide range of adjustable parameters that influence fiber morphology and orientation. This adaptability makes it a promising approach to address challenges like low cellularization efficiency, one of the critical hurdles in the development of 3D-engineered tissues, particularly when pore sizes are either excessively small or large.[127] Nowadays, several electrospinning variants have been developed, such as coaxial electrospinning,[103,128] wet electrospinning,[129] in-line blending,[130] and emulsion electrospinning[131] each offering specific advantages. To emulate the distinctive mechanical behavior of native T/Ls, scaffold designs have incorporated features that replicate, to some degree, their wavy architecture.

In a study conducted by Wu and coworkers[100] a nanofibrous poly(p-dioxanone)/silk fibroin (PPDO/SF) scaffold was fabricated by electrospinning, followed by a thermal ethanol treatment to induce a wavy fibrous morphology (Figure 6). Biological tests on tenocytes showed that

2688268x, 0, Downloaded from https://onlinelibrary.wiley.com/doi/10.1002/VIW.20250063 by CochraneItalia, Wiley Online Library on [16/10/2025]. See the Terms and Conditions (https://onlinelibrary.wiley.com/terms-and-conditions) on Wiley Online Library for rules of use; OA articles are governed by the applicable Creative Commons License

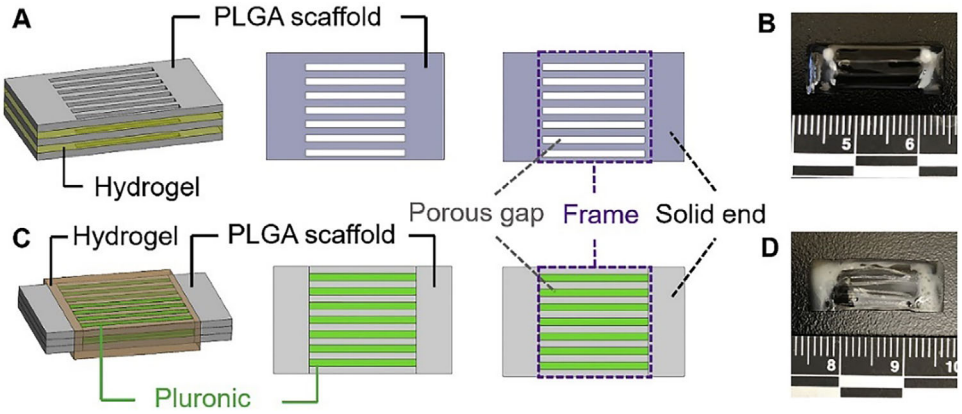

FIGURE 5 Schematic representation and close-up photographs of 3D-printed PLGA composite scaffolds with different configurations. Reproduced with permission from Jiang et al.[98]

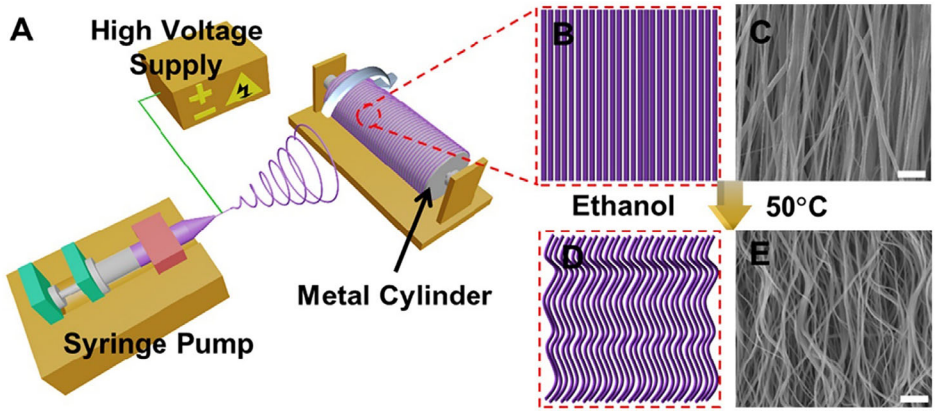

FIGURE 6 Schematic representation of the electrospinning process and subsequent ethanol and thermal treatment, resulting in aligned fibers with a wavy pattern. Reproduced with permission from Wu et al.[100]

the incorporation of SF improved cell adhesion and proliferation, while in vivo subcutaneous implantation in rats reduced the inflammatory response, highlighting the scaffold's biocompatibility. Taking a different fabrication strategy, Camarero-Espinosa and colleagues[102] achieved wavy fiber architectures by thermally shrinking PLA films supporting aligned electrospun mats. The structural modification influenced cell behavior significantly: cells cultured on wavy scaffolds formed aggregates, deposited a rich ECM enriched in fibronectin and COLI, and exhibited elevated expression of TNMD compared with aligned scaffolds.

Expanding on the role of biochemical modifications, Tu and their team[101] fabricated poly(L-lactide-co-ε-caprolactone) (PLCL)/collagen I nanoyarn scaffolds using an electrospinning setup equipped with a basin and a water vortex. By crosslinking fibromodulin with collagen, they successfully promoted the tenogenic differentiation of human adipose-derived stem cells (hASCs), underscoring the potential of biochemical modifications in guiding cellular behavior.

In a related study, Tu's group[103] employed coaxial electrospinning to fabricate a PLGA/chitosan tubular scaffold modified with soluble T ECM (sTECM). PLGA served as the core structure, while PLGA and sTECM formed the outer shell. Biomechanical testing at 12 weeks postimplantation in rat Achilles Ts showed a Young's modulus of approximately 600 MPa, suggesting that both biochemical and structural modifications synergistically contribute to scaffold function. However, a direct comparison between these approaches is needed to fully assess their relative advantages. Similarly, Sheng and colleagues[104] focused on fiber alignment by developing a biomimetic electrospun sheath composed of PCL/Gelatin to encase the patellar T in a rabbit model. Histological examination at 8 weeks postimplantation demonstrated favorable orientation of collagen fibrils and spindle nuclei of fibroblasts, further corroborating that the alignment of the fibers is an important factor in tissue regeneration. Although these results align with those of Tu's nanoyarn scaffolds, the different materials and fabrication techniques employed raise questions

2688268x, 0, Downloaded from https://onlinelibrary.wiley.com/doi/10.1002/VIW.20250063 by CochraneItalia, Wiley Online Library on [16/10/2025]. See the Terms and Conditions (https://onlinelibrary.wiley.com/terms-and-conditions) on Wiley Online Library for rules of use; OA articles are governed by the applicable Creative Commons License

about the optimal approach for achieving a functional regeneration.

Another key aspect in the electrospinning-based scaffold design is the effect of fiber diameter on cell responses. Baldwin and colleagues[105] investigated the effect PDO electrospun scaffold topography on the transcriptional response of healthy and diseased T fibroblasts. Scaffolds with aligned fibers exceeding 2000 nm in diameter led to an upregulation of genes involved with DNA and cell replication and downregulated those linked with inflammation. These results are consistent with previous studies highlighting the influence of fiber alignment, but they also introduce fiber diameter as an additional parameter for modulating cell behavior. In another innovative approach, Song's team[106] developed an immunoregulatory PCL scaffold functionalized with a layer-by-layer coating of SF linked with mechano-growth factor via click chemistry. In a rat Achilles TI model, inflammation was undetectable 28 days postimplantation, demonstrating the scaffold's ability to mitigate foreign body reactions. Seeking to enhance mechanical properties, Li and their group[107] sought to enhance the mechanical properties of electrospun scaffolds by fabricating a nanofibrous PCL/methacrylated poly(trimethylene carbonate) (PTMC–MA) composite. Their results showed that increasing PTMC–MA content significantly improved mechanical performance, with scaffolds containing a 1:3 ratio of PCL/PTMC–MA exhibiting a stress at break of 23.80 ± 3.44 MPa, comparable to native Ts.

Among the various electrospinning strategies, particular attention has been devoted to the fabrication of aligned nanofiber bundles or yarns.[132] Their elongated, cylindrical geometry more closely reflects that of native T/Ls, which themselves are composed of parallel collagen bundles organized into hierarchical fascicles. To meet the complex three-dimensional architecture and functional demands of T/L tissue, scalable manufacturing approaches such as twisting, braiding, or knitting have been explored to assemble these nanofiber units into robust, clinically relevant grafts.[133]

In a work by Pauly and colleagues,[108] PCL-aligned nanofiber sheets were produced via electrospinning. Rectangular sections of these mats were then tightly rolled into cylindrical bundles, preserving both fiber orientation and interfiber porosity. This assembly produced bundles with mechanical properties including elastic modulus, yield stress, and yield strain, comparable to those of the native anterior cruciate L (ACL).

In a subsequent study by the same group,[109] hierarchical scaffolds were fabricated from aligned electrospun PCL nanofibers. Flat nanofiber mats were cut into narrow strips and tightly rolled to form cylindrical bundles, which were then grouped and secured to create a multi-bundle fiber region. To replicate the functional integration with bone, each end of the bundle assembly was embedded within solid PCL blocks using a solvent-casting process. The resulting construct combined nanoscale fiber alignment with macroscale bundle architecture, resulting in a scaffold that reproduced both the hierarchical morphology and the anatomical dimensions of the native ACL.

Transitional interfaces, such as the T-to-bone enthesis[134] and the MJT, are essential for efficient force transfer and overall musculoskeletal performance. An ideal scaffold should not only emulate the hierarchical micro- and nanoscale architecture of these interfaces, but also reflect their spatially graded cellular, biochemical, and mechanical characteristics.[135] The work by Zhao and fellow researchers[110] reported the fabrication of hierarchical, stretchable, and stiff fibrous scaffolds by combining PCL microfibers with chitosan (ChS) nanofibers through a staggered electrospinning process, aimed at supporting rotator cuff T repair. Compared with pure CS scaffolds, the PCL–CS composites displayed markedly greater tensile strength and failure strain, while also exhibiting higher stiffness than PCL-based scaffolds. The incorporation of CS improved scaffold hydrophilicity, water uptake, and degradation rate, and promoted superior fibroblast adhesion and proliferation. At the T–bone interface, scaffolds using the composite scaffolds achieved higher mechanical strength, stiffness, and failure strain than those obtained with PCL alone. Restoring MTJ presents an equally demanding challenge. In their study, Su and colleagues[111] developed a three-dimensional MTJ model incorporating a biomimetic "M-type" interface. The scaffold was produced from electrospun nanofiber yarns arranged through an interwoven weaving method, resulting in highly aligned fibers that promoted cell elongation and orientation. The M-type interface was designed to reproduce the structural transition between muscle and T regions, improving spatial organization and functional interaction of cells across the junction. To address the challenge of coculturing myocytes and tenocytes under distinct but adjacent conditions, the scaffold was incorporated into a microfluidic platform capable of delivering separate media to each zone. The compartmentalized MTJ-on-a-chip system offered a controlled environment for studying interface biology and has potential applications in drug testing. Likewise, Iwasaki's obtained aligned electrospun PCL fibers which served as a substrate for the coculture of human myoblasts and tenocytes to investigate MTJ formation in vitro. The influence of 10% cyclic strain and direct coculture was assessed, revealing that mechanical stimulation promoted greater cell elongation and upregulated MTJ-specific gene expression. Notably, characteristic native MTJ proteins such as paxillin and collagen type XXII were detected under these combined conditions.

2688268x, 0, Downloaded from https://onlinelibrary.wiley.com/doi/10.1002/VIW.20250063 by CochraneItalia, Wiley Online Library on [16/10/2025]. See the Terms and Conditions (https://onlinelibrary.wiley.com/terms-and-conditions) on Wiley Online Library for rules of use; OA articles are governed by the applicable Creative Commons License

Despite its widespread use, electrospinning suffers several limitations, among which the cytotoxicity[136] due to solvents residual within the electrospun fibers is the most frequent. This risk can be mitigated by using low-boiling points or low-toxicity solvents. Alternatively, the investigation of water-based solvents systems is a viable path for environmentally friendly manufacturing processes. Additionally, integrating advanced drying systems such as heated airflows or vacuum-assisted collection chambers could further enhance solvent removal. Another main obstacle is the inherently low yield of production of electrospinning, making it difficult to scale up to industrial applications. A multineedle electrospinning system is a valid alternative to address this issue by increasing the throughput while maintaining a high fiber quality.

4.3 | Melt electrowriting

MEW is an emerging fabrication technique that like electrospinning uses an electrical field through which molten polymers can deposit into fibers in a layer-by-layer manner,[112] with diameters ranging from 2 to 50 μm.[137] The standard setup includes a heated polymer delivery system, a three-axis positioning mechanism for an accurate material deposition, and a high-voltage power supply for generating a potential between the delivery system and the collector. The electric field created between the printhead and the collector charges the molten droplet,[93] and when these charges exceed the surface tension of the material, a Taylor cone is generated, propelling the molten jet toward the collector.[138] Several studies have explored the potential of MEW in T/L TE by optimizing fiber architectures and mechanical properties.

Von Witzleben and colleagues[139] fabricated a rectangular PCL scaffold via the MEW technique, followed by a type I collagen coating extracted from rat tail (Figure 7). Their comparative analysis of fiber architecture demonstrated that rhombohedral pore geometries enhanced cell alignment of hASCs more effectively than traditional grid structures. This shows the important role of pore geometry in regulating cell behavior, with certain designs having the ability to promote cell alignment and function. To approximate the biomechanical behavior of human T/Ls, Hochleitner and their team[113] fabricated poly(e-caprolactone-co-acryloyl carbonate) scaffolds with a sinusoidal architecture by MEW at speeds below the critical translation threshold, ensuring the fibers retained their sinusoidal morphology. These scaffolds demonstrated cytocompatibility with murine L929 cells and mimic the characteristic toe region seen in T stress–strain curves.

Despite its potential, MEW faces significant challenges related to ink formability. A crucial problem concerns the viscosity control of the ink. Low-viscosity inks are easy to extrude and to manipulate but collapse when deposited, while high-viscosity inks are difficult to extrude and may not respond adequately to the electric field.[140] Therefore, finding an optimal balance between these extremes is essential for improving MEW accuracy and reliability. One potential solution to this problem involves shape memory polymers that dynamically adjust their viscosity in response to external stimuli.[138,141] This approach would enable more precise control over the extrusion process thereby enhancing overall accuracy and reliability.

4.4 | Hybrid fabrication techniques

The integration of different fabrication techniques allows researchers to retain the advantages of each individual methodology while mitigating their respective limitations. In this way, the fabrication of scaffolds is custom designed for either single or multiple tissue types.[142] For instance, while textile techniques allow for the fabrication of macroscopic structures with defined patterns and porosities[143], the incorporation of electrospinning enables the integration of nanoscale fibers within such constructs, enhancing their functional properties.[115,116,144,145]

Cai and their group[114] explored this synergy by combining electrospinning with traditional textile weaving. They employed SF/PLLA nanofiber yarns as weft and commercial PLLA microfiber yarns as warp producing a nanofibrous scaffold with a plain-weaving structure. These scaffolds promoted cell adhesion, alignment, proliferation, and the preservation of tenocyte phenotype in vitro. Biomechanical tests performed 6 months postsurgery in rats Achilles T defect model revealed a failure load of 44.2 ± 6.9 N, surpassing that of native Ts (39.9 ± 4.3 N). Building on this concept, Xie and fellow researchers[115] introduced an innovative micro–nano hierarchical scaffold designed to mimic the natural organization of collagen fibrils. Using electrospinning, they created aligned PLGA nanoyarns loaded with Fibrin which were then braided onto a triple-helix structure. This design promoted T cells alignment and proliferation in vivo. Shalumon and coauthors[116] fabricated a scaffold by collecting aligned PCL electrospun fibers around a commercial suture. Three of these single yarns were braided together and surface modified with heparin grafting. Retrieved samples of rabbit extensor digitorum T at 6 weeks postimplantation exhibited a failure load of 16.58 ± 3.05 N, demonstrating its mechanical viability as an alternative to autologous T grafts.

2688268x, 0, Downloaded from https://onlinelibrary.wiley.com/doi/10.1002/VIW.20250063 by CochraneItalia, Wiley Online Library on [16/10/2025]. See the Terms and Conditions (https://onlinelibrary.wiley.com/terms-and-conditions) on Wiley Online Library for rules of use; OA articles are governed by the applicable Creative Commons License

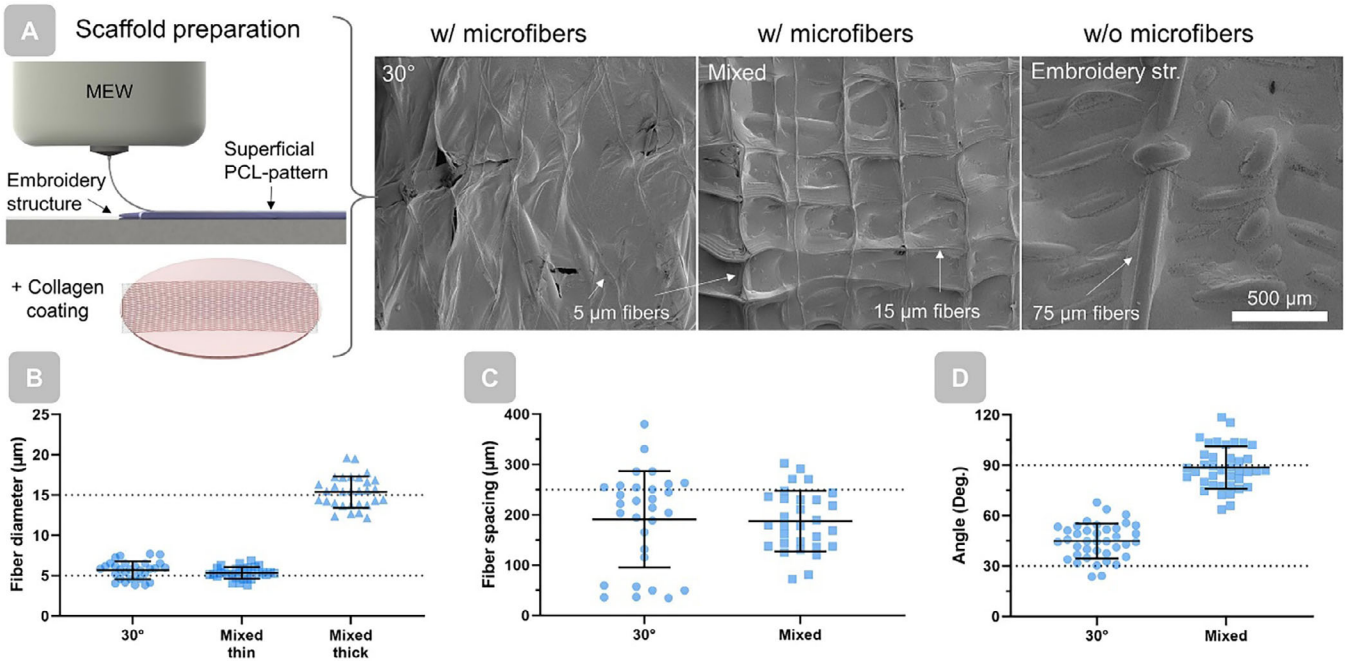

FIGURE 7 Schematic representation of the scaffold fabrication process, combining melt electrowriting (MEW) to create embroidery structures with a superficial PCL pattern and collagen coating (A). Quantitative analysis of fiber diameter (B), fiber spacing (C), and fiber alignment angle (D) for different scaffold designs. Reproduced with permission from von Witzleben et al.[139]

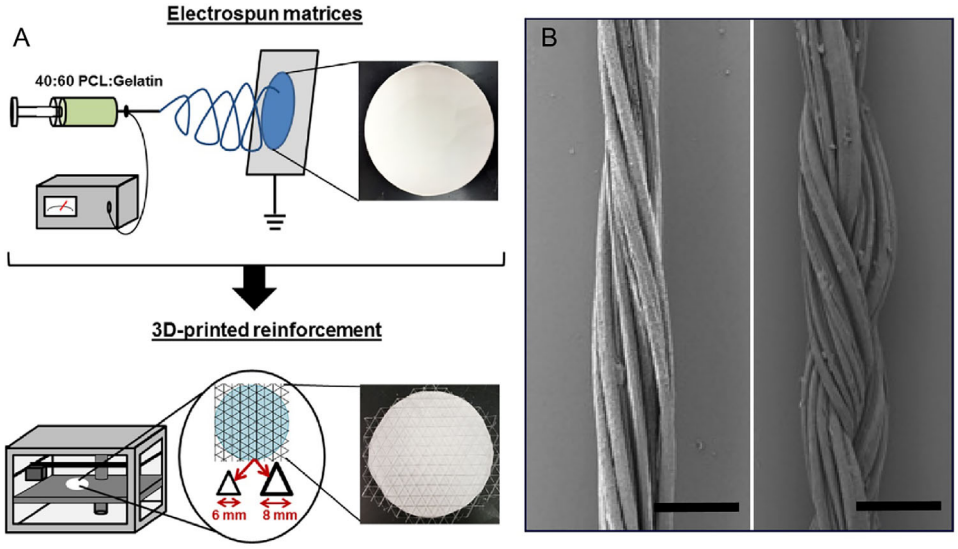

FIGURE 8 Examples of scaffolds developed through advanced hybrid fabrication techniques. (A) 3D-printed reinforced electrospun scaffold. Reproduced with permission from Pensa e al., licensed under Creative Commons Attribution 4.0 International.[117] (B) Scaffold created by braiding three yarns, which were twisted from electrospun fibers. Scale bar: 200 µm. Readapted from Laranjeira et al.[145]

Another example of the combination of technologies is the assay conducted by Pensa's group[117] in which hybrid patches were obtained by printing a PLA mesh onto PCL/Gelatin electrospun mats (Figure 8A). In vivo functional tests in a rat bone defect model showed no inflammatory response 20-week postimplantation. A graded scaffold composed of PLGA and PCL was produced by Criscenti and colleagues[94] through a two-step fabrication process designed to replicate the multitissue architecture of the native L-to-bone insertion. The L-like region was formed by electrospinning PLGA, while the bone-mimicking region was created via 3D fiber deposition of PCL. An intermediate fibrocartilaginous zone was obtained by combining the two techniques.

2688268x, 0, Downloaded from https://onlinelibrary.wiley.com/doi/10.1002/VIW.20250063 by CochraneItalia, Wiley Online Library on [16/10/2025]. See the Terms and Conditions (https://onlinelibrary.wiley.com/terms-and-conditions) on Wiley Online Library for rules of use; OA articles are governed by the applicable Creative Commons License

Uniaxial tensile testing revealed distinct mechanical behaviors for each region, with the electrospun PLGA segment exhibiting a significantly higher Young's modulus than the 3D-printed PCL segment. In the graded region, the mechanical response was largely influenced by the PCL component. Similarly, the work by Alkaissy and fellow researchers[118] integrates electrospinning and 3D printing to produce soft–hard biphasic scaffolds for potential use in rotator cuff repair. The approach involves embedding an electrospun PDO cuff within a porous PCL block during the 3D printing process. The cuff's insertion area was designed to match the supraspinatus T footprint, and its strength was scaled by increasing the number of electrospun filaments from 9 to 270, reaching an average load capacity of 227 N. Mechanical performance was influenced by filament configuration, whereas biological assessments confirmed the noncytotoxicity of both scaffold components and their ability to support T cell growth on the cuff and bone cell growth on the block.

The work of Micalizzi and coworkers[119] aimed to design and fabricate an innovative multimaterial and multiscale scaffold capable of inducing cells into a graded enthesis-like tissue comprising a T/L region and a bone region. The scaffold designed to replicate bone tissue was fabricated using FDM of PCL, where to reproduce the anisotropic fiber orientation typical of native T/Ls, PLGA was processed by electrospinning. The resulting scaffold supported MSCs adhesion and promoted their differentiation into both osteoblasts and tenocytes. Furthermore, the interface between PCL and PLGA demonstrated mechanical integrity by withstanding tensile strains during testing.

Taken together, the findings of several studies indicate a promising potential for combining electrospinning with other fabrication approaches to bridge scaffolds toward the native T/L's structural and mechanical properties. A recurring theme among them is the employment of aligned nanofibers, whether woven, braided, or incorporated into hierarchical structures, to guide cell alignment and improve mechanical performance. This alignment appears to be an important part of enhancing tenocyte proliferation and phenotype maintenance. In the near future, it can be expected that more techniques of this kind will be applied.

4.5 | Decellularized tissue-derived scaffolds

Decellularization is a process that removes cell components from the ECM without disrupting its inherent structure and mechanical integrity. It begins with the extraction of tissues from an animal donor, followed by treatment with specific reagents and wash solutions to eliminate cell material, resulting in a protein-based matrix. The resulting ECM can be seeded with cells for transplantation as a regenerative medicine application.[146] Ts[120,121,147] and other connective tissues[123] are common sources for decellularization-derived scaffolds, which possess several advantages including reduced immunogenicity and enhanced biocompatibility.[148] One of the primary benefits of decellularization over synthetic fabrication methods, such as electrospinning and 3D printing, is the ability to retain the native ECM architecture (Figure 9).[95] This biomimetic structure provides a biologically relevant environment that can facilitate cell attachment, proliferation, and differentiation, features that are difficult to fully replicate using synthetic approaches.

Several studies have demonstrated the regenerative potential of decellularized T scaffolds. In a study undertaken by Niveditha and coresearchers[120] decellularization of rat Achilles T was accomplished using tri(n-butyl) phosphate. The T was used as a platform for further seeding with rat ASCs and for the delivery of *Tinospora cordifolia extract*, used in many ayurvedic preparations. Cell viability and proliferation assays demonstrated increased proliferation rates, with stem cells adopting a spindle-shape morphology typical of tenocytes. In a related approach, Cui and colleagues[121] employed bovine T sheets functionalized with collagen-binding domain extracellular vesicles from TSPCs. Biomechanical tests on regenerated rat Achilles Ts 12 weeks postimplantation revealed a failure load of 110 N, denoting the mechanical strength of the implant. Further innovations have been aimed at improving the mechanical properties of decellularized scaffolds. Wang and colleagues[122] applied a double cross-linked CS modification to enhance the mechanical properties of decellularized mussel adductor muscle scaffolds. Histological evaluations performed after implantation on rats' Achilles T defect model indicated that the engineered T may be beneficial toward tissue remodeling and regeneration. However, it remains unclear how the CS modification would fare in long-term in vivo applications, particularly in terms of maintaining scaffold integrity under dynamic loading conditions typical of Ts. The research team led by Chen et al[123] fabricated a bioactive collagen I scaffold (BCS) from porcine connective tissue seeded with human T stem cells (hTSCs) exposed to cyclic uniaxial loading. The work progressed to a pilot human safety study, confirming the feasibility in mini-open or arthroscopic rotator cuff repair (Figure 10).

The limited availability of donor tissue, along with the biological variability of native T/Ls restrict shape tailoring and scalability for clinical applications. Moreover, the decellularization process is capable of compromising ECM integrity, leading to the loss of essential components,

2688268x, 0, Downloaded from https://onlinelibrary.wiley.com/doi/10.1002/VIW.20250063 by CochraneItalia, Wiley Online Library on [16/10/2025]. See the Terms and Conditions (https://onlinelibrary.wiley.com/terms-and-conditions) on Wiley Online Library for rules of use; OA articles are governed by the applicable Creative Commons License

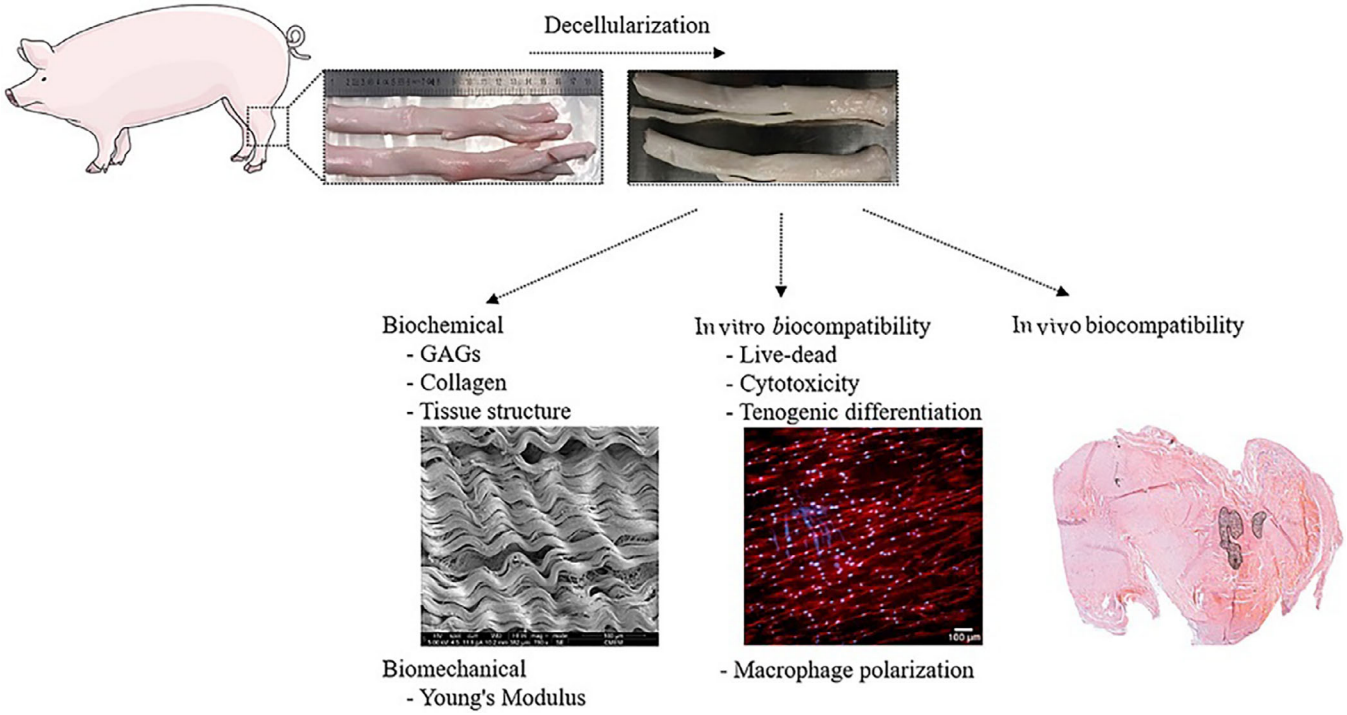

FIGURE 9 Schematic illustration of the fabrication process of decellularized tendon scaffolds (DTSs). Reproduced with permission from Dede Eren et al.[148]

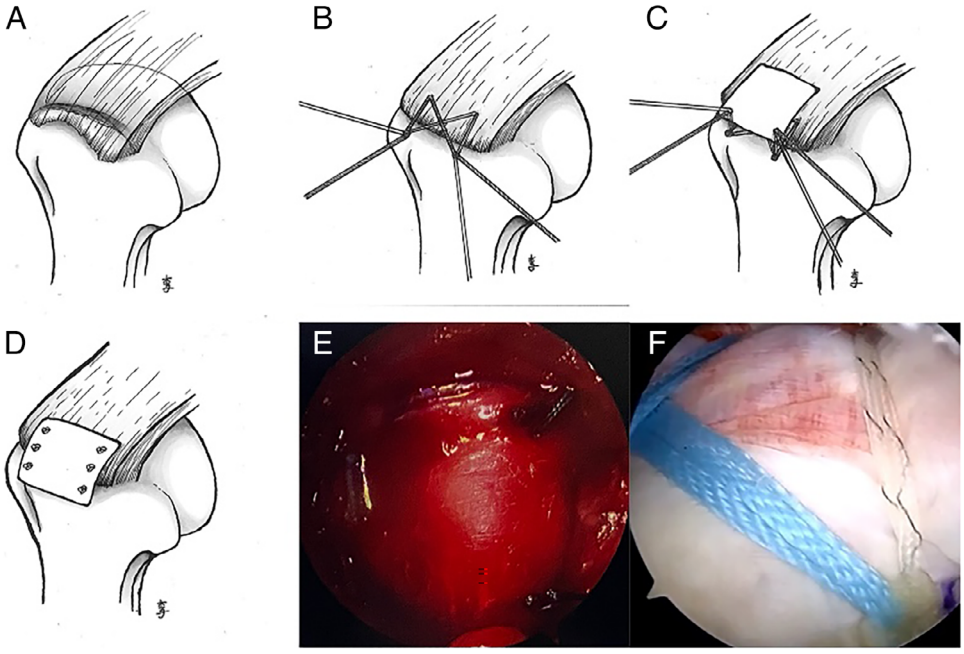

FIGURE 10 Schematic and intraoperative acquisitions of on-lay bioactive collagen scaffold (BCS) repair of human supraspinatus tendon. Reproduced with permission from Chen et al.[123]

including GAGs and growth factors. Such limitations can lead to the reduction of the scaffold's bioactivity, which can affect its long-term functionality.

To deal with these challenges the development of cutting-edge strategies is fundamental. Decellularized ECM has been investigated as bio-ink for 3D bioprinting.[149] Additionally, the integration of decellularized ECM with other biofabrication techniques offers the potential to deliver bioactive molecules and cells, which enhances the regenerative potential of scaffolds.

2688268x, 0, Downloaded from https://onlinelibrary.wiley.com/doi/10.1002/VIW.20250063 by CochraneItalia, Wiley Online Library on [16/10/2025]. See the Terms and Conditions (https://onlinelibrary.wiley.com/terms-and-conditions) on Wiley Online Library for rules of use; OA articles are governed by the applicable Creative Commons License

5 | CELL SOURCES

Cells, as basic units of all living tissues, represent a central element in TE since they constitute the biological framework in which ECM components are synthesized. Cells in scaffolds create dynamic microenvironments during repair and promote cell retention at the injury site. This aspect prevents undesired migration to surrounding tissues, which could potentially result in unintended side effects. Advances in cell manipulation and differentiation have significantly broadened the range of available options, allowing more specific and effective regenerative approaches[150] (Table 3). However, the clinical translation of cell-based approaches remains in its early stages. Currently, a limited number of phase 1 and 2 clinical trials are either in progress or have been completed for the cell treatment of T/Ls disorders.[151] Among the most commonly used cell types in T/L TE are tenocytes,[152] fibroblasts, and stem cells that possess the ability to differentiate into T-like cells.[153]

5.1 | Stem cells

Stem cells offer a highly versatile solution in T/L TE, owing to their ability for self-renewal and differentiation into multiple mesodermal lineages, including osteoblasts (bone), CHs (cartilage), tenocytes (T)[17] when exposed to specific biochemical and mechanical cues. Of special interests are MSCs, which have attracted significant interest based on their high proliferation rates and high biosynthetic activity. The use of either autologous or allogeneic MSCs presents this great trade-off: with allogeneic MSCs, off-the-shelf availability and large-scale expansion can be achieved but with risks of pathogen transmission and immune rejection. Several studies have explored the use of MSCs in combination with advanced biomaterials and mechanical stimulation. For instance, Li's research team[154] fabricated a PCL tubular scaffold via e-jetting and coated it with alginate before seeding it with hMSCs. Subjecting the construct to cyclic uniaxial strain (0.5 Hz, 3%) significantly upregulated T-specific protein expression and promoted cell alignment along the scaffold's longitudinal axis. Similarly, Chae and colleagues[149] employed 3D bioprinting techniques, embedding hBMSCs in a bio-ink composed of decellularized T/Ls tissues. PCL was incorporated to provide mechanical stability, and live/dead staining showed high cell viability with an elongated morphology indicative of tenogenic differentiation. Yang and team[155] developed collagen tubular scaffolds through counter-rotating extrusion and seeded them with BMSCs. The aligned collagen fibers not only replicated the structural organization of native Ts but also promoted tenogenic differentiation by guiding cell elongation along the fiber direction. Nevertheless, BMSCs are not without limitations. Ectopic bone formation has been reported,[164] along with inferior strength compared with uninjured Ts. In addition, the aspiration procedure involving the harvest of MSCs is invasive and often painful, thus limiting its clinical applicability.[165] In light of these challenges, TSPCs have emerged as an attractive alternative since; unlike BMSCs, TSPCs are naturally predisposed toward tenogenesis.

The existence of a pool of stem cells in Ts can be confirmed in multiple Ts and ligaments from different species.[29,166,167] Ning and coworkers[147] demonstrated the regenerative potential of TSPCs by first seeding them onto a decellularized T substrate and then taking the construct through a second decellularization process. The resulting composite was then used to assess its ability in providing support for BMSC migration, proliferation, and tenogenic differentiation, with favorable outcomes. Meanwhile, Kim and colleagues[160] investigated the influence of nanotopographical cues on TSPC behavior by fabricating a PCL patch via capillary force lithography. Immunofluorescence analysis revealed that TSPCs underwent alignment along the patterned surface, forming organized cell–cell interactions indicative of tenogenic commitment. However, TSPCs present limitations that hinder their use on a large-scale for treating T/Ls injuries. The limited quantity of cells present in T tissue requires a significant volume of source material to secure an adequate number of cells.

5.2 | Fibroblasts

Fibroblasts are the predominant cell type in connective tissues and are responsible in the synthesis of ECM proteins such as type I and III collagen,[168] fibronectin, and PGs and are typically characterized by their spindle- or stellate-shaped morphology, which is contingent upon the specific tissue in which they are located. Dermal fibroblasts and tenocytes share a common mesodermal origin, which makes fibroblasts an attractive alternative for T repair.[99,104,151,153] Their ease of extraction (which requires only a small skin biopsy) minimizes donor site morbidity compared with T-derived cells. Clinical trials have shown promising results, as injections of autologous dermal fibroblast have reduced pain in patients with refractory patellar tendinopathy.[169]

Xuan and team[131] fabricated a PLLA scaffold with a core-shell structure by emulsion electrospinning, incorporating L-arginine (L-Arg) and HA in order to support different phases of T healing. Mouse fibroblasts exhibited significantly higher proliferation rates on the Arg/HA-modified scaffold.

2688268x, 0, Downloaded from https://onlinelibrary.wiley.com/doi/10.1002/VIW.20250063 by CochraneItalia, Wiley Online Library on [16/10/2025]. See the Terms and Conditions (https://onlinelibrary.wiley.com/terms-and-conditions) on Wiley Online Library for rules of use; OA articles are governed by the applicable Creative Commons License

TABLE 3 Summary of the main cell types used in scaffolds for tendon repair.

Scaffold composition	Cells	Cell source	Animal model	Implant site	Outcome	References
PCL	MSCs	Human	–		Increased production of COL1, DCN, TNC, TNMD	154
PCL	BMSCs	Human	Mouse	Subcutaneous implantation	Increased expression in *SCX, TNMD, COL1A1, COL3A1*	149
Collagen	BMSCs	Rat	Rat	Achilles tendon	Increased expression in *Col1a1, Bgn, Tnc, Scx, Tnmd, Dcn*	155
Decellularized tendon	BMSCs	Rat	–	–	Increased expression in *Scx, Tnmd, Tnc, Col1, Col3, Thbs4*	147
PCL/ChS	MSCs	Human	–	–	Cell elongation along the direction of fibers; enhanced proliferation	156
PCL	MSCs	Human	Rat	Achilles tendon	Increased expression in FN, DCN, TNC, SCX TNMD	157
Silk/Gelatin	MSCs	Goat	Mouse	Subcutaneous implantation	Increased expression In SCX, TNMD, COL1 and COL3	158
Collagen I-III (DuRepair™)	BMSCs	Pig	Rat	Achilles tendon	Improved biomechanical properties	159
PCL	TSCs (supraspinatus tendon)	Human	Rabbit	Supraspinatus tendon	Increased production of COL1, OCN, FN	160
PLLA	Fibroblasts (adipose tissue)	Mouse	Rat	Achilles tendon	Enhanced proliferation	131
PDLLA/Collagen I	Tenocytes	Human	Rabbit	Achilles tendon	Cell elongation along the direction of fibers	161
MnO2-Modified Decellularized Tendon	Tenocytes	Rat	Rat	Patellar tendon	Increased expression in SCX, TNMD, MKX	162
PCL/Collagen I	Tenocytes	Rat	–	–	Cell elongation along the direction of fibers; enhanced proliferation	163

Abbreviations: PCL, polycaprolactone; MSCs, mesenchymal stem cells; COL1, collagen type I; DCN, decorin; TNC, tenascin C; TNMD, tenomodulin; BMSCs, bone marrow mesenchymal stem cells; SCX, scleraxis; COL1A1, collagen type I alpha 1 chain; COL3A1, collagen type III alpha 1 chain; BGN, biglycan; COL3, collagen type III; THBS4, thrombospondin 4; TSCs, tendon-derived stem cells; ChS, chitosan; OCN, osteocalcin; FN, fibronectin; PLLA, poly (L-lactic acid); PDLLA, poly(D,L-lactide).

One of the major concerns in the use of fibroblasts is the potential fibroproliferative response, which could lead to the deposition of excessive scar tissue formation rather than a functional T/L regeneration.[170]

5.3 | Tenocytes

As resident T cells, tenocytes hold particular advantages in T/L TE due to their specialized function in ECM maintenance. Tenocytes already express the genes and proteins required for T homeostasis, unlike stem cells, eliminating the need for directed differentiation.[171] Furthermore, they do not pose the risk of teratoma formation, a concern associated with pluripotent stem cells.[172]

Maghdouri-White and colleagues[161] evaluated the potential of tenocyte-seeded scaffolds by developing an electrospun PDLLA-collagen I scaffold coated with platelet-rich plasma. In vitro testing confirmed tenocyte alignment along the scaffold's fibers, and in vivo implantation in a rabbit Achilles TI model revealed early remodeling at 16 weeks and complete integration at

2688268x, 0, Downloaded from https://onlinelibrary.wiley.com/doi/10.1002/VIW.20250063 by CochraneItalia, Wiley Online Library on [16/10/2025]. See the Terms and Conditions (https://onlinelibrary.wiley.com/terms-and-conditions) on Wiley Online Library for rules of use; OA articles are governed by the applicable Creative Commons License

52 weeks, suggesting the long-term viability of tenocyte-based constructs.

However, tenocyte-based therapies face several barriers to clinical translation. Isolation of tenocytes requires a T biopsy, an invasive procedure with the risk of donor site morbidity. Moreover, tenocytes exhibit limited proliferative capacity which requires extended culture periods to obtain therapeutically relevant cell numbers. This limitation, when compared with more expandable cell sources such as MSCs or fibroblasts, represents a substantial constraint in terms of mass clinical implementation.

A key takeaway from the studies discussed here is the widespread appreciation that cell behavior is greatly influenced by scaffold architecture and mechanical stimulation. Through multiple studies, aligned topographical cues and dynamic mechanical loading allow enhanced tenogenic differentiation, regardless of the cell type used.

6 | BIOACTIVE COMPONENTS

Over the last decade, there has been a growing body of research exploring the functionality of bioactive compounds in TE.[173] To this end, multiple strategies have been developed to enhance T/L regeneration by delivering bioactive molecules including hormones,[174,175] nanoparticles,[176,177] drugs or growth factors all of which play a crucial role in the modulation of the immune response at the injury site[129] (Table 4). The incorporation of bioactive components into scaffolds is not limited to a single method: researchers have explored different techniques, such as surface coating, encapsulation within the scaffold itself, direct chemical bonding with the scaffold material,[125] and loading within micro- or -nanoparticles as carriers for the delivery bioactive molecules at the target site.

6.1 | Growth factors

Growth factors are signaling molecules, typically proteins or steroid hormones, involved in the regulation of cell processes such as proliferation, differentiation, and growth.[190] Among these, TFG-β is a protein superfamily that exhibits a multifaceted function in wound healing, through promotion of inflammation during initial stages and enabling ECM deposition as healing occurs.[191,192]

Donderwinkel and team[178] investigated the effects of TGF-β3 supplementation on tenogenic differentiation of hBMSCs cultured on 3D printed poly(D,L-lactic acid ethylene glycol-D,L-lactic acid) and GelMA hydrogel scaffolds, widely used in musculoskeletal TE.[193] Their findings indicated that samples supplemented with 5 ng/mL TGF-β3 and subjected to 3% of intermittent cyclic uniaxial strain exhibited optimal tenogenic differentiation, with increased SCX and COL1A1 expression and improved ECM organization.

Similarly, the FGF family regulates a broad spectrum of biological processes, including proliferation, inflammation, angiogenesis, and collagen synthesis.[130,144,184]

Building on the bioaffinity with heparin, Darshan and coworkers[130] encapsulated FGF-2 within a gelatin/PCL/heparin electrospun scaffold. The scaffold effectively maintained the tenocyte phenotype, promoting enhanced expression of key tenogenic markers during in vitro culture (Figure 11).

Bone morphogenic proteins (BMPs), also known as growth differentiating factors belong to the TGF-β superfamily and regulate chemotaxis, proliferation, ECM synthesis, and tenogenic differentiation during T healing.[194] BMP levels are elevated during the early phases of T healing and gradually decline over time.[195] In the context of embryogenic development, BMP-12 and BMP-13 have been observed to promote the expression of elastin and collagen I, thereby contributing to the development of mechanically robust Ts.[196] Rinoldi and coworkers[177] fabricated electrospun meshes using a combination of PCL, polyamide 6 (PA6), and mesoporous silica particles, subsequently functionalizing them with BMP-12. Results demonstrated that BMSCs cultured on BMP-12-enriched scaffolds exhibited enhanced TNMD expression, indicating improved tenogenic differentiation.

This aligns with findings from Güner and team,[129] who investigated BMP-14′s role in the tenogenic differentiation of hADSCs seeded on a dual-phase PCL (shell)/PCL–gelatin (core) scaffold fabricated via rotary jet electrospinning and wet electrospinning. Supplementation with 100 ng mL^{-1} proved to be most effective on the expression of TNMD, total collagen deposition, COLIII deposition, and cell migration.

Beyond BMPs and FGFs, the use of combined mechanical and biochemical stimulation has been explored to optimize T/L regeneration. Jayasree and their laboratory[144] developed a multiscale fibrous scaffold by integrating electrospinning with textile techniques. They loaded FGF-2 into collagen-poly(vinyl alcohol) (PVA) nanofibers, which were further blended with electrospun PCL microfibers to form braided scaffolds. Their work demonstrated a synergistic effect between mechanical stimulation (applied at 0.5 Hz for 3 h/day with 5% elongation) and growth factor delivery, leading to increased expression of COLI, COLIII, TNC, BGN, and FN, as confirmed by qPCR analysis.

PDGFs is another growth factor group relevant in T/L TE. PDGFs are dimeric growth factors held together by disulfide bonds. These factors have several isoforms, each being a dimer of two polypeptide chains, either AA, BB, or

2688268x, 0, Downloaded from https://onlinelibrary.wiley.com/doi/10.1002/VIW.20250063 by CochraneItalia, Wiley Online Library on [16/10/2025]. See the Terms and Conditions (https://onlinelibrary.wiley.com/terms-and-conditions) on Wiley Online Library for rules of use; OA articles are governed by the applicable Creative Commons License

TABLE 4 Overview of the key bioactive components used in scaffolds for tendon repair.

Bioactive component	Type	Scaffold composition	Fabrication technique	Cell source	Outcome	References
TGF-β3	Growth factor	(P(LA-EG-LA))–GelMa	3D Printing	Human BMSCs	Increased expression in *SCX* and *COL1A1*	178
FGF-2	Growth factor	Gelatin/PCL/heparin	Electrospinning	Rabbit tenocytes	Increased expression in COL1, BGN, TNC	130
BMP-12	Growth factor	PCL/PA6	Electrospinning	Human BMSCs	Increased production of TNMD	177
BMP-14	Growth factor	PCL/gelatin	Wet electrospinning/ rotary jet electrospinning	Human ASCs	Increased production of TNMD, COL3	129
FGF-2	Growth factor	PCL/collagen	Electrospinning/textile technologies	Rabbit tenocytes	Increased expression in COL1, COL3, TNC, BGN, FN	144
PDGF-BB	Growth factor	DegraPol® (polyester urethane)	Coaxial electrospinning	Rabbit tenocytes	Increased production of COL1, COL3	128
RSV	Drug	GG	Hydrogel preparation	–	Enhanced vasculature formation and collagen deposition	179
Celecoxib	Drug	CCBP	Electrospinning	–	Local stimulation of growth factors around the wound site	180
Naproxen	Drug	AUP/PCL	Electrospinning	Human fibroblasts	High cell viability after 7 days	181
Methylprednisolone	Drug	PLGA	Electrospinning	–	Antibacterial activity against *E. coli and S. aureus* Reduction in the formation of adhesions (for 25% methylprednisolo loaded PLGA scaffolds)	182
AgNPs	Filler	PLA	3D printing	Human TSCs	Antibacterial activity against *E. coli and S. aureus* Increased expression in *SCX, COL1, TNMD*	176

(Continues)

2688268x, 0, Downloaded from https://onlinelibrary.wiley.com/doi/10.1002/VIW.20250063 by CochraneItalia, Wiley Online Library on [16/10/2025]. See the Terms and Conditions (https://onlinelibrary.wiley.com/terms-and-conditions) on Wiley Online Library for rules of use; OA articles are governed by the applicable Creative Commons License

TABLE 4 (Continued)

Bioactive component	Type	Scaffold composition	Fabrication technique	Cell source	Outcome	References
Bioactive glass	Filler	PU/silk fibroin	Electrospinning	BMSCs	Increased production of ALP	183
Bioactive glass	Filler	PCL/PGS	Electrospinning/3D printing	Mouse fibroblasts	High cell viability after 7 days for scaffolds with 10% of bioactive glass	184
Sr–HT	Filler	UHMWPE/PVA/ gelatin	Extrusion	Rat TSCs	Hindered expression in *Col1, Col3, Scx,Tnmd, Tnc* Good collagenous tissue ingrowth in vivo	185
miRNA	Posttranscriptional gene regulator	engineered miRNA plasmid/-PLGA nanoparticles embedded in HA hydrogel	Hydrogel casting	Chicken tenocytes	Reduced tendon adhesion	186
miRNA	Posttranscriptional gene regulator	PLGA nanoparticles	Double emulsion solvent evaporation	Chicken tenocytes	Reduced tendon adhesion	187
miR-126	Posttranscriptional gene regulator	PELCL	Emulsion electrospinning	HUVECs	Enhanced endothelializa-tion	188
miR-21-3p	Posttranscriptional gene regulator	Scaffold free approach	NA	HUMSCs	Reduced tendon adhesion	189

Abbreviations: TGF-β3, transforming growth factor-β3; (P(LA-EG-LA)), poly(D,L-lactic acid ethylene glycol-D,L-lactic acid); GelMA, gelatin methacrylate; SCX, scleraxis; COL1A1, collagen type i alpha 1 chain; FGF-2, fibroblast growth factor-2; PCL, polycaprolactone; COL1, collagen type I; BGN, biglycan; TNC, tenascin C; BMP, bone morphogenic protein; PA6, polyamide 6; BMSCs, bone marrow mesenchymal stem cells; TNMD, tenomodulin; ASC, adipose-derived stem cells; COL3, collagen type III; FN, fibronectin; PDGF-BB, platelet-derived growth factor-BB; RSV, rosuvastatin calcium; GG, gellan gum; CCBP, celecoxib, collagen, bupivacaine, and PLGA; AUP, acrylate-endcapped urethane-based polymer; AgNPs, silver nanoparticles; PLA, poly(lactic acid); TSCs, tendon-derived stem cells; PU, polyurethane; ALP, alkaline phosphatase; PGS, poly (glycerol sebacate); Sr–HT, strontium-doped hardystonite(Sr–Ca2ZnSi2O7); UHMWPE, ultra-high molecular weight polyethylene; PVA, poly(vinyl alcohol); PELCL, poly(ethylene glycol)-b-poly(L-lactide-co-e-caprolactone); HUVECs, human umbilical vein endothelial cells; HUMSCs, human umbilical cord mesenchymal stem cells.

a combination of the two. Furthermore, PDGFs stimulate the migration and proliferation of several cell populations involved in T/Ls regeneration such as fibroblasts, tenocytes, and MSCs.[197]

Evrova and colleagues[128] investigated the use of the polyesterurethane DegraPol® for the sustained delivery of PDGF-BB. They employed two electrospinning techniques, coaxial and emulsion electrospinning to incorporate the growth factor within the polymeric solution, enabling a controlled release over 30 days. In vivo studies using a rat Achilles T defect model demonstrated the potential of these scaffolds, with tubular scaffolds obtained via coaxial electrospinning leading to a twofold increase in the maximum load of healed Ts after 3 weeks postsurgery.

Although these studies highlight the potential of growth factor incorporation into scaffolds, significant challenges exist. The clinical application of growth factors is limited due to high costs, short half-life, and uncertainties regarding optimal dosages.[198] Given the involvement of multiple growth factors in T/Ls regeneration as described above, their simultaneous use is a strategic solution to better replicate the natural healing cascade. Although this strategy holds some promise in maximizing the regenerative outcome, it also significantly increases treatment costs and complexity.

6.2 | Pharmacological agents

Systemic or local administration is the routes for delivery of pharmacological agents which help to modulate inflammation, pain, and ECM remodeling. Systemic

2688268x, 0, Downloaded from https://onlinelibrary.wiley.com/doi/10.1002/VIW.20250063 by CochraneItalia, Wiley Online Library on [16/10/2025]. See the Terms and Conditions (https://onlinelibrary.wiley.com/terms-and-conditions) on Wiley Online Library for rules of use; OA articles are governed by the applicable Creative Commons License

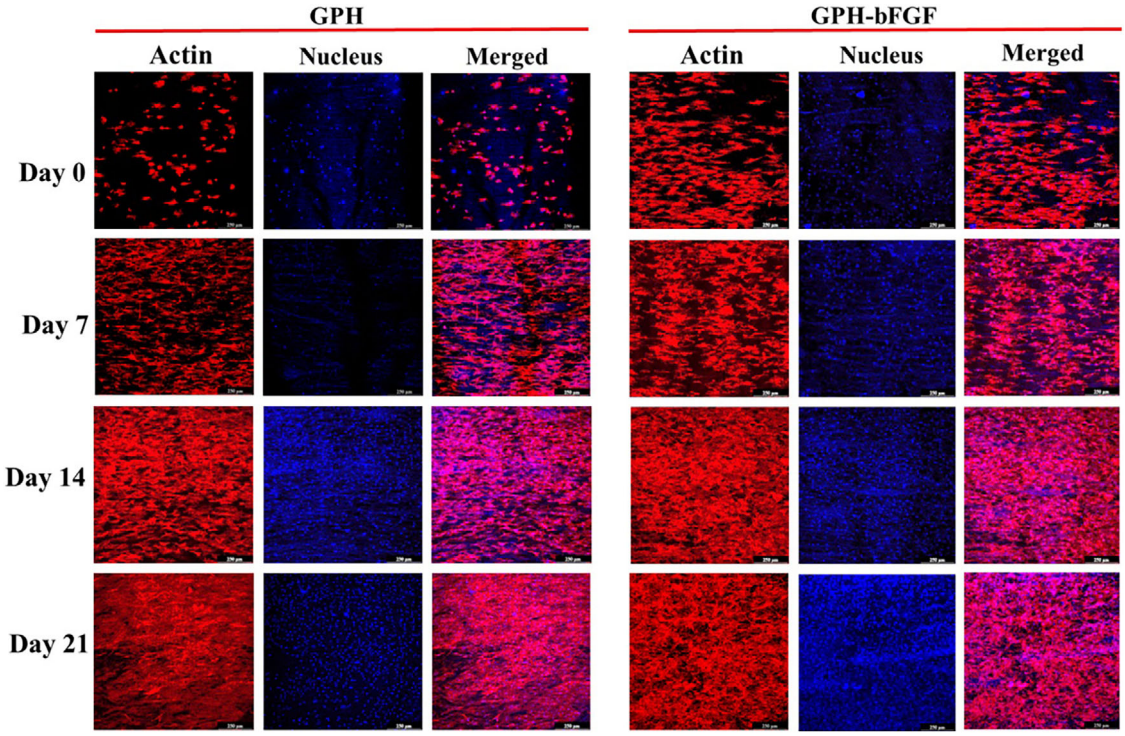

FIGURE 11 Nuclear and actin cytoskeleton staining of tenocyte-seeded gelatin–PCL–heparin (GPH) and GPH–bFGF scaffolds. Scale bar = 250 μm. Reproduced with permission from Darshan et al.[130]

administration methods, such as intravenous, intramuscular, and oral routes, ensure widespread drug distribution but could lead to off-target effects.[179] To mitigate side effects and improve drug effectiveness, it is essential to develop carriers that preserve the drug's functions, protect it from decomposition or denaturation, and deliver it to the target site.[199] Conversely, local delivery through biomaterials provides precise control over drug release, minimizing systemic exposure while enhancing therapeutic outcomes.[200] Local delivery strategies include hydrogels, films, sponges, fibers, and injectable carriers like cross-linkable hydrogels and nanoparticles.[179,201] Adel and coworkers[179] explored the use of a bi-polymeric hydrogel scaffold for the localized delivery of rosuvastatin calcium (RSV) as an inhibitor of farnesyl pyrophosphate, a known wound healing inhibitor. RSV was incorporated into a scaffold made of gellan gum and a secondary polymer (either κ-carrageenan, carboxymethyl cellulose, or PVA). Functional tests on rat Achilles Ts showed enhanced vasculature formation and high rates of collagen expression. A common approach among recent studies involves the incorporation of bioactive agents directly into the polymeric solution before electrospinning, ensuring homogeneous drug distribution within the scaffold and allowing for controlled, sustained release profiles. Yu and fellow researchers[180] developed an electrospun scaffold incorporating Celecoxib, a widely used analgesic, blended with collagen, bupivacaine (a potent local anesthetic), and PLGA. In vitro release profiles indicated a sustained celecoxib release over 30 days, while in vivo studies on an Achilles T rat model guaranteed a release of 28 days. The prolonged drug delivery profile suggests a viable strategy for managing inflammation and pain following injury. Likewise, Pien and colleagues[181] designed a tubular scaffold composed of an Acrylate-endcapped urethane-based polymer (AUP)/PCL blend loaded with Naproxen, an anti-inflammatory agent, and HA, specifically designed to reduce scar tissue formation. In vitro biocompatibility assays employing human fibroblasts confirmed the scaffold noncytotoxic nature, whereas ex vivo biomechanical testing on a cadaveric sheep flexor digitorum profundus T model revealed substantial improvements of the mechanical properties with the reinforced AUP530:PCL construct. Zuhour and coworkers[182] incorporated methylprednisolone, known for its anti-inflammatory, antifibrotic, and immunosuppressant properties, into a PLGA polymeric solution before electrospinning. Drug release analysis showed an initial burst release within the first 24 h, followed by a sustained release profile that ensured gradual drug delivery with most of the drug released by the 14th day. Notably, the MP/PLGA scaffold exhibited antibacterial activity against *E. coli* and *S. aureus*. Implantation of the 25% MP-loaded PLGA scaffold resulted in reduced adhesion formation compared with control Ts, highlighting the

2688268x, 0, Downloaded from https://onlinelibrary.wiley.com/doi/10.1002/VIW.20250063 by CochraneItalia, Wiley Online Library on [16/10/2025]. See the Terms and Conditions (https://onlinelibrary.wiley.com/terms-and-conditions) on Wiley Online Library for rules of use; OA articles are governed by the applicable Creative Commons License

potential advantages of integrating anti-inflammatory and antimicrobial properties into T repair scaffolds.

One common challenge in many applications discussed in this paragraph is the need for accurate control over the drug release rate. Furthermore, residual empty carriers postdrug depletion could potentially trigger inflammation, making it essential to eliminate them alongside the drug release. To address these challenges, personalized design of drug release modifiers that can be combined with a drug and assist in regulation of the drug release independently of polymer degradation kinetics offer a promising solution.

6.3 | Fillers

Polymer composites are advanced materials designed to improve mechanical, biological, and functional properties by blending a reinforcement phase within a polymeric matrix.[202] The matrix maintains cohesion between interfaces and facilitates the transfer of forces experienced by the composite. The resulting material is characterized by high heterogeneity and often exhibits anisotropic properties. Several factors affect these features, including the type of matrix and filler, the shape and proportion of the filler, the quality of the interface, and the manufacturing processes employed. Various fillers like titanium dioxide, hydroxyapatite, and bioactive glass (BG), can be incorporated into scaffolds to improve their functional properties.[203]

To confer antibacterial properties Silva and coworkers[176] integrated 0.5 wt.% of functionalized graphene nanoplatelets decorated with silver nanoparticles ((f-EG)+Ag) into a medical-grade PLA matrix. The resulting filaments were used to fabricate cylindrical scaffolds via 3D printing, further seeded with hTSCs. As expected, silver nanoparticles exhibited antibacterial activity against *S. aureus* and *E. coli*. In addition, the presence of (f-EG)+Ag significantly upregulated the expression of the tenogenic markers *SCX*, *TNMD*, and *COL1*, highlighting the scaffold's potential in promoting T regeneration.

BG represents a class of reactive materials recognized for their biocompatibility and ability to bond with mineralized bone tissue.[204,205] It is generally made up of Na_2O, CaO, P_2O_5, and SiO_2, with SiO_2 content kept below 55%. The properties of BG can be customized by modifying the concentrations of its components to trigger specific biological responses.

Touré and team[184] incorporated BG into a PCL/poly(glycerol sebacate) (PGS) blend, using a combination of 3D printing and electrospinning techniques (Figure 12). The electrospun mats provided a reinforcement to the 3D-printed patches due to strong interfacial adhesion between the layers, resulting in a in Young's

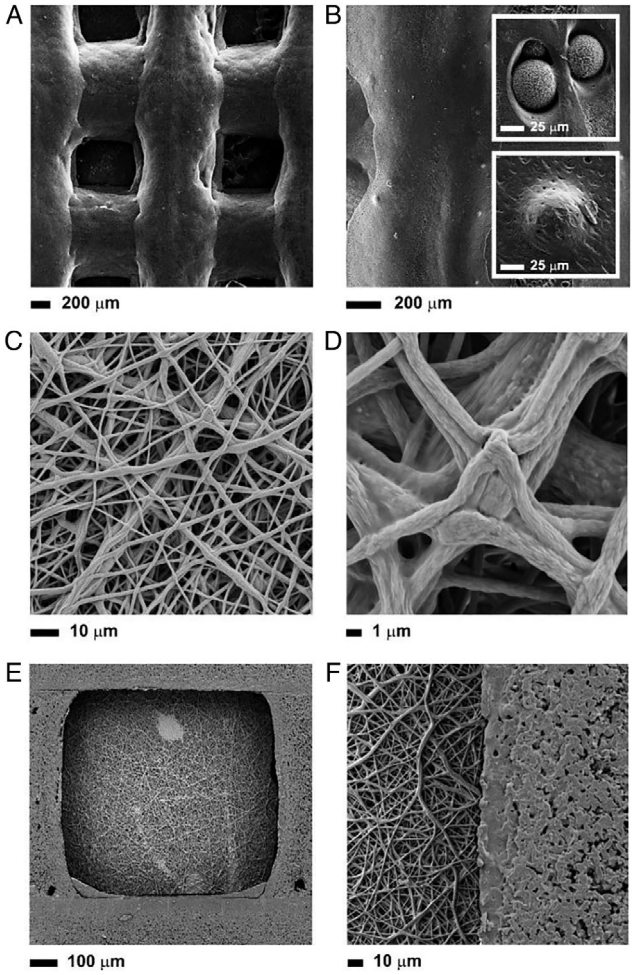

FIGURE 12 SEM images at different magnifications depicting: (A and B) 3D-printed scaffolds with BG microspheres either embedded within the polymer matrix or exposed on the surface (see insets); (C and D) the composite scaffold coated with electrospun PCL–PGS mats; (E and F) the composite scaffold surface without the electrospun fiber layer. Reproduced with permission from Tourè et al.[184]

modulus of 311 ± 20 MPa for scaffolds containing 10% w/w BG. In vitro assays with mouse fibroblasts demonstrated the highest cell viability at day 7 in scaffolds containing 10% BG.

Strontium–hardystonite (Sr–Ca2ZnSi2O7, Sr–HT) is a bioactive calcium silicate with potential applications in musculoskeletal TE. Although native T/Ls contain less than 0.2% inorganic material,[206] trace amounts of metal ions such as calcium, silicon, zinc, and strontium have been found to be essential in the growth, repair, and maintenance of musculoskeletal tissues, including T/Ls.[207] No and team[185] investigated the incorporation of Sr–HT into a hydrogel, which was injected into an ultra-high molecular weight polyethylene fibrous scaffold and subsequently pultruded it through a circular channel to fabricate a fiber-reinforced hydrogel construct. In vitro studies using

2688268x, 0, Downloaded from https://onlinelibrary.wiley.com/doi/10.1002/VIW.20250063 by CochraneItalia, Wiley Online Library on [16/10/2025]. See the Terms and Conditions (https://onlinelibrary.wiley.com/terms-and-conditions) on Wiley Online Library for rules of use; OA articles are governed by the applicable Creative Commons License

TSPCs suggested that Sr–HT might inhibit tenogenic differentiation, while in vivo implantation in a rat patellar T model demonstrated substantial collagenous tissue ingrowth within the scaffold 6 weeks postimplantation.

6.4 | miRNA

miRNAs are small noncoding RNA molecules, typically 18–25 nucleotides in length, that regulate gene expression at a posttranscription level by guiding the RNA-induced silencing complex to target messenger RNAs, thereby promoting their degradation or inhibiting their translation.[208] Through this mechanism, miRNAs exert fine-tuned control over a wide array of biological processes, including cell differentiation, proliferation, apoptosis, migration, and tissue homeostasis. Because miRNAs are naturally expressed within cells, therapeutic approaches can be designed to either restore a lost function or suppress an aberrant one. Replacement is generally achieved using synthetic miRNA mimics, whereas inhibition is accomplished through specific miRNA inhibitors.[209] In the context of T/L TE, miRNAs have attracted considerable interest due to their ability to modulate ECM remodeling, regulate the expression of T-specific transcription factors, and influence key signaling pathways involved in mechanotransduction and inflammation. Naked miRNAs exhibit poor cellular uptake due to their negative charge, short systemic half-life, and susceptibility to rapid degradation or inactivation by blood nucleases, as well as the risk of both undesired off-target and on-target effects.[210] miRNAs delivery systems can be broadly classified into viral and nonviral vectors.[211] Viral vectors, including retroviruses, lentiviruses, adenoviruses, and adeno-associated viruses, are widely used in clinical protocols for their high transfection efficiency; however, safety concerns such as immunogenicity and mutagenicity limit their broader application. Nonviral carriers such as lipid-based nanoparticles, polymer-based systems, and inorganic nanoparticles offer several advantages, including lower immunogenicity, and versatility in functionalization with targeting ligands. The choice of delivery platform depends on the route of administration and the intended therapeutic goal. Important miRNAs for T/Ls repair include miR-21-5p, which promotes T cell proliferation and differentiation while modulating fibrosis, miR-210, known to modulate angiogenesis 165, and miR-135a that promotes the tenogenic differentiation of TDSCs.[212] Nevertheless, despite the growing body of evidence supporting their therapeutic relevance, the clinical translation of miRNA-based strategies for T/L repair remains hindered by challenges, including the achievement of precise, tissue-specific delivery and the fine-tuning of dosage to balance efficacy.[213]

7 | ANIMAL MODELS

The successful clinical translation of T/L TE strategies depends on the selection of relevant preclinical models. The appropriate selection of an animal model in proof-of-concept studies includes a careful evaluation of significant characteristics: anatomical site, surgical accessibility, biomechanical properties, and overall clinical relevance.[214]

Rodents, particularly rats and mice, are among the most employed animal species[180] due to their small dimensions and ease of handling that facilitate reproducible experimental techniques. Additionally, their cost effectiveness compared with larger animal species makes them an attractive option for preclinical research. However, the advantages they provide are somewhat limited by their small T sizes and differences in biomechanical loading that present a significant barrier toward direct clinical translatability. As a result, larger animals such as rabbits,[104] dogs, sheep, pigs, and horses have gained increasing relevance due to their closer resemblance to human T anatomy.[214,215] Among these species, rabbits offer a practical compromise between small and large animal models, having Ts large enough for surgical manipulation and biomechanical analysis. Rabbit flexor Ts are very close to human Ts in terms of diameter and the presence of a synovial sheath, thus of extremely high relevance in both flexor and Achilles T research. Nonetheless, species differences must be considered; for example, rabbits typically maintain greater knee flexion in ventral recumbency, and their posterior knee structures exhibit distinct biomechanical properties.[215]

Dogs are also a useful model due to their anatomical and functional similarities to human flexor Ts. Furthermore, their ability to participate in postoperative mobilization exercises adds translational relevance. However, ethical concerns and their status as companion animals have led to a decline in their use for experimental research.[216]

Sheep, particularly skeletally mature ewes are widely used in rotator cuff injuries, given the anatomical and functional similarities between the ovine infraspinatus T and the human supraspinatus T.[217] Their size and shape adds value of being compatible with a variety of noninvasive imaging such as ultrasound. However, due to the high cost of procurement and maintenance, and breed-dependent variability, makes standardizing outcomes a challenge.

Pigs represent a relevant large-animal model, particularly for ACL research (Figure 13). The porcine ACL exhibits mechanical properties similar to its human counterpart, including comparable load-to-failure and stiffness, which are significantly lower in small animal models. However, anatomical differences need to be considered, such as the larger cross-sectional area and distinct

2688268x, 0, Downloaded from https://onlinelibrary.wiley.com/doi/10.1002/VIW.20250063 by CochraneItalia, Wiley Online Library on [16/10/2025]. See the Terms and Conditions (https://onlinelibrary.wiley.com/terms-and-conditions) on Wiley Online Library for rules of use; OA articles are governed by the applicable Creative Commons License

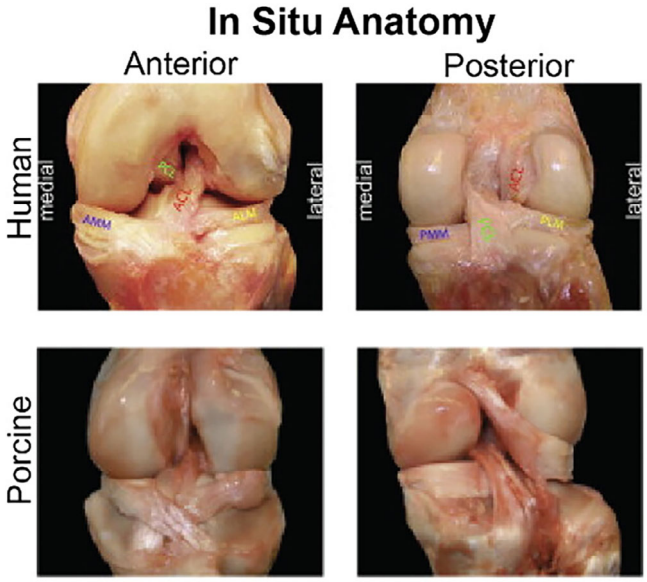

FIGURE 13 Comparative in situ anatomy of the human (top row) and porcine (bottom row) knee joints, viewed from anterior (left) and posterior (right) perspectives. Adapted from Little et al.[216]

insertion sites of the porcine ACL. Nevertheless, structural measurements, including overall ACL length and tibial plateau width, are comparable between pigs and humans, and therefore suitable for translational studies.[218]

The equine model has a distinct set of advantages that maximizes the utility when studying high-load Ts such as the flexor digitorum superficialis T, which shares functional similarities with the human Achilles T.[219] Like humans, horses rely on energy-storing Ts for high-speed locomotion. However, its application is hampered by significant logistical challenges, including high maintenance costs, specialized housing requirements, and ethical considerations.

Ultimately, the choice of an animal model should be carefully aligned with the specific research objectives, taking into consideration the biological relevance as well as the practical feasibility. In many cases, a strategic approach that integrates multiple models may be necessary to bridge the gap between basic research and clinical translation.

8 | CONCLUSIONS AND FUTURE CHALLENGES

Further improvements in T/L TE will not be without challenges. The main drawback in this regard is the ability to replicate the complex multiscale structure of T/L tissue. In terms of microstructure, their complex hierarchical organization extends across multiple scales, ranging from the nanoscale to the macroscale. With such complexity, no single biomaterial can fully replicate the structural and functional characteristics of native T/Ls tissues. Hence, composite scaffolds that include multiple scale-specific components would provide a mechanism to guide the cell behavior toward a desired end and hence facilitate regeneration. In addition, one of the main barriers in widespread clinical applications is the scaling up of the scaffold fabrication. Demand for tissue-engineered T/L constructs is now growing, and most solutions are still in an experimental stage; therefore, establishing high-throughput processes for scaffold biofabrication will be crucial. Addressing this issue requires interdisciplinary collaboration among bioengineers, clinicians, and material scientists to drive technological advancements and optimize translational potential.

Last, the other major limitation lies in the predominant reliance on small animal models in preclinical studies. Although rodents are used as models for genetic and molecular research, their size makes it difficult to investigate major T/L defects. Therefore, greater efforts should be directed toward developing standardized large animal models with better methods of evaluation and stricter quality control.

The ongoing worldwide interest in T/L TE suggests that the field will evolve toward increasingly sophisticated strategies aimed at achieving more effective and comprehensive T/L regeneration. With the development of new technologies and interdisciplinary collaborations, the implementation of innovations into clinical settings may become a reality in the near future.

AUTHOR CONTRIBUTIONS

Francesca Romano: Conceptualization; writing—original draft; writing—review and editing. **Roberto Di Gesù:** Conceptualization; writing—review and editing; visualization; and supervision. **Francesco Lopresti:** Conceptualization; writing—review and editing; visualization. **Vincenzo La Carrubba:** Visualization.

ACKNOWLEDGEMENTS

We express our gratitude to the Ri.MED Foundation for their support, which was fundamental in the development, preparation, and publication of this comprehensive review article. The Ri.MED foundation commitment to advancing scientific research and innovation in the biomedical field has significantly contributed to the successful completion of this work.

CONFLICT OF INTEREST STATEMENT

The authors declare no conflict of interest.

ORCID

Roberto Di Gesù https://orcid.org/0000-0001-6196-643X

2688268x, 0, Downloaded from https://onlinelibrary.wiley.com/doi/10.1002/VIW.20250063 by CochraneItalia, Wiley Online Library on [16/10/2025]. See the Terms and Conditions (https://onlinelibrary.wiley.com/terms-and-conditions) on Wiley Online Library for rules of use; OA articles are governed by the applicable Creative Commons License

REFERENCES

1. N. L. Leong, J. L. Kator, T. L. Clemens, A. James, M. EnamotoIwamoto, J. Jiang, *J. Orthop. Res.* **2020**, *38*, 7.
2. E. Bianchi, M. Ruggeri, S. Rossi, B. Vigani, D. Miele, M. C. Bonferoni, G. Sandri, F. Ferrari, *Pharmaceutics* **2021**, *13*, 89.
3. F. Wu, M. Nerlich, D. Docheva, *EFORT Open Reviews* **2017**, *2*, 332.
4. M. O'Brien, in *Tendon Injuries: Basic Science and Clinical Medicine* (Eds: N. Maffulli, P. Renström, W. B. Leadbetter), Springer, London **2005**, 12.
5. M. N. Hafeez, N. d'Avanzo, V. Russo, L. Di Marzio, F. Cilurzo, D. Paolino, M. Fresta, B. Barboni, H. A. Santos, C. Celia, *Stem Cells Int.* **2021**, *1*, 2021.
6. M. Wójtowicz, D. Ciechanowicz, B. Ufnalska, K. Rękawek, Ł. Kołodziej, *Chir. Narzadow Ruchu Ortop. Pol.* **2023**, *88*, 172.
7. O. Drogomiretskiy, L. Hjelm, K. Millonig, S. Rush, T. M. Chappell, C. Clifford, *Foot Ankle Surg.* **2022**, *2*, 100250.
8. L. Bobzin, R. R. Roberts, H. J. Chen, J. G. Crump, A. E. Merrill, *Development* **2021**, *148*, 1.
9. M. L. Killian, *Semin. Cell Dev. Biol.* **2022**, *123*, 64.
10. J. Apostolakos, T. J. S. Durant, C. R. Dwyer, R. P. Russell, J. H. Weinreb, F. Alaee, K. Beitzel, M. B. Mccarthy, M. P. Cote, A. D. Mazzocca, *Muscles Ligaments Tendons J.* **2014**, *4*, 333.
11. R. Gottardi, K. Moeller, R. Di Gesù, R. S. Tuan, M. Van Griensven, E. R. Balmayor, *Front. Mater.* **2021**, *8*, 1.
12. F. Snow, C. O'Connell, P. Yang, M. Kita, E. Pirogova, R. J. Williams, R. M. I. Kapsa, A. Quigley, *APL Bioeng.* **2024**, *8*, 021505.
13. K. A. Shama, M. A. Turner, H. B. Broadaway, E. L. Aikman, W. L. Stoppel, B. L. Taylor, *Curr. Opin. Biomed. Eng.* **2024**, *30*, 100532.
14. L. C. Rocha-Braga, J. Pimentel Neto, I. Gomes, A. P. Ciena, *Front. Physiol.* **2025**, *16*, 1.
15. K. Allen, E. Feria-Arias, C. Kreulen, E. Giz, in *Sports Injuries of the Foot and Ankle* (Eds: G. L. Canata, P. d'Hooghe, K. J. Hunt, G. M. M. J. Kerkhoffs, U. G. Longo), Cambridge University Press, Cambridge **2018**, 306.
16. A. Aparecida de Aro, B. de Campos Vidal, E. R. Pimentel, *Micron* **2012**, *43*, 205.
17. M. Schneider, P. Angele, T. A. H. Järvinen, D. Docheva, *Adv. Drug Delivery Rev.* **2018**, *129*, 352.
18. H. Tempfer, A. Traweger, *Front. Physiol.* **2015**, *6*, 1.
19. G. G. Schulze-Tanzil, M. Delgado Cáceres, R. Stange, B. Wildemann, D. Docheva, *Bone Jt. Res.* **2022**, *11*, 561.
20. D. Thesis, Advancing the Cell Culture Landscape Advancing the Cell Culture Landscape: The Instructive Potential of Artificial and Natural. 2021.
21. S. Zhang, W. Ju, X. Chen, Y. Zhao, L. Feng, Z. Yin, X. Chen, *Bioact Mater* **2022**, *8*, 124.
22. I. Tresoldi, F. Oliva, M. Benvenuto, M. Fantin, L. Masuelli, R. Bei, A. Modesti, *Muscles Ligaments Tendons J* **2013**, *3*, 2.
23. I. Silva Barreto, M. Pierantoni, M. Hammerman, E. Törnquist, S. Le Cann, A. Diaz, J. Engqvist, M. Liebi, P. Eliasson, H. Isaksson, *Matrix Biol.* **2023**, *115*, 32.
24. M. R. Citeroni, M. C. Ciardulli, V. Russo, G. Della Porta, A. Mauro, M. El Khatib, M. Di Mattia, D. Galesso, C. Barbera, N. R. Forsyth, N. Maffulli, B. Barboni, *Int. J. Mol. Sci.* **2020**, *21*, 6726.
25. A. J. Lomas, C. N. M. Ryan, A. Sorushanova, N. Shologu, A. I. Sideri, V. Tsioli, G. C. Fthenakis, A. Tzora, I. Skoufos, L. R. Quinlan, G. O'Laighin, A. M. Mullen, J. L. Kelly, S. Kearns, M. Biggs, A. Pandit, D. I. Zeugolis, *Adv. Drug Delivery Rev.* **2015**, *84*, 257.
26. S. P. Magnusson, K. M. Heinemeier, M. Kjaer, *Adv. Exp. Med. Biol.* **2016**, 920.
27. J. G. Snedeker, J. Foolen, *Acta Biomater.* **2017**, *63*, 18.
28. C. N. M. Ryan, D. I. Zeugolis, *Adv. Ther.* **2020**, *3*, 1.
29. D. Docheva, S. A. Müller, M. Majewski, C. H. Evans, *Adv. Drug Delivery Rev.* **2015**, *84*, 222.
30. M. J. Mienaltowski, S. M. Adams, D. E. Birk, *Tissue Eng., Part A* **2013**, *19*, 199.
31. H. Liu, S. Zhu, C. Zhang, P. Lu, J. Hu, Z. Yin, Y. Ma, X. Chen, H. Ouyang, *Cell Tissue Res.* **2014**, *356*, 287.
32. M. van Vijven, S. L. Wunderli, K. Ito, J. G. Snedeker, J. Foolen, *J. Orthop. Res.* **2021**, *39*, 1561.
33. K. Spanoudes, D. Gaspar, A. Pandit, D. I. Zeugolis, *Trends Biotechnol.* **2014**, *32*, 474.
34. S. Vermeulen, A. Vasilevich, D. Tsiapalis, N. Roumans, P. Vroemen, N. R. M. Beijer, A. Dede Eren, D. Zeugolis, J. De Boer, *Acta Biomater.* **2019**, *83*, 277.
35. S. Yoshida, N. Hasegawa, Y. Kobayashi, A. Miyachi, H. Sakaki, K. Nishikawa, Y. Moriguchi, S. Furuta, C. Maekawa, I. Urushibara, S. Kawasaki, *2015 IEEE International Symposium on Radio-Frequency Integration Technology, RFIT 2015 - Proceedings*, **2016**.
36. J. Wang, Q. Guo, B. Li, *J. Hand Ther.* **2012**, *25*, 133.
37. P. F. Lozano, M. Scholze, C. Babian, H. Scheidt, F. Vielmuth, J. Waschke, B. Ondruschka, N. Hammer, *Sci. Rep.* **2019**, *9*, 1.
38. S. Ruiz-Alonso, M. Lafuente-Merchan, J. Ciriza, L. Saenz-delBurgo, J. L. Pedraz, *J. Controlled Release* **2021**, *333*, 448.
39. V. Turitto, S. M. Slack, Handbook of Biomaterial Properties, Second ed. **2016**.
40. C. Rinoldi, E. Kijeńska-Gawrońska, A. Khademhosseini, A. Tamayol, W. Swieszkowski, *Adv. Healthcare Mater.* **2021**, *10*, 2001305.
41. T. A. L. Wren, S. A. Yerby, G. S. Beaupré, D. R. Carter, *Clin. Biomech.* **2001**, *16*, 245.
42. C. N. Maganaris, J. P. Paul, *J. Biomech.* **2002**, *35*, 1639.
43. T. D. O'Brien, N. D. Reeves, V. Baltzopoulos, D. A. Jones, C. N. Maganaris, *J. Biomech.* **2010**, *43*, 1190.
44. M. Kongsgaard, C. H. Nielsen, S. Hegnsvad, P. Aagaard, S. P. Magnusson, *Clin. Biomech.* **2011**, *26*, 772.
45. G. A. Lichtwark, A. M. Wilson, *J. Exp. Biol.* **2005**, *208*, 4715.
46. C. N. Maganaris, J. P. Paul, *J. Physiol.* **1999**, *521*, 307.
47. E. Morales-Orcajo, R. Becerro De Bengoa Vallejo, M. Losa Iglesias, J. Bayod, *Clin. Biomech.* **2016**, *37*, 1.
48. C. W. Kolz, T. Suter, H. B. Henninger, *Clin. Biomech.* **2015**, *30*, 940.
49. A. Race, A. A. Amis, *J. Biomech.* **1994**, *27*, 13.
50. V. Burgio, S. Casari, M. Milizia, F. Sanna, G. Spezia, M. Civera, M. Rodriguez Reinoso, A. Bertuglia, C. Surace, *Biomech. Model. Mechanobiol.* **2023**, *22*, 1645.
51. B. Wu, Y. Fu, H. Shi, B. Yan, R. Lu, S. Ma, B. Markert, *BioMed. Eng. OnLine* **2018**, *17*, 172.
52. J. D. Hewitt, R. R. Glisson, F. Guilak, T. P. Vail, *J. Arthroplasty* **2002**, *17*, 82.
53. S. Siegler, J. Chen, C. D. Schneck, *IEEE Eng Med Biol Soc Annu. Conf.* **1988**, *10*, 622.
54. J. Zhang, G. Lu, Z. You, *Composites, Part B* **2020**, *201*, 108340.

2688268x, 0, Downloaded from https://onlinelibrary.wiley.com/doi/10.1002/VIW.20250063 by CochraneItalia, Wiley Online Library on [16/10/2025]. See the Terms and Conditions (https://onlinelibrary.wiley.com/terms-and-conditions) on Wiley Online Library for rules of use; OA articles are governed by the applicable Creative Commons License

55. R. Gatt, M. Vella Wood, A. Gatt, F. Zarb, C. Formosa, K. M. Azzopardi, A. Casha, T. P. Agius, P. Schembri-Wismayer, L. Attard, N. Chockalingam, J. N. Grima, *Acta Biomater.* **2015**, *24*, 201.
56. C. V. Nagelli, A. Hooke, N. Quirk, C. L. De Padilla, T. E. Hewett, M. Van Griensven, M. Coenen, L. Berglund, C. H. Evans, S. A. Müller, *Eur. Cells Mater.* **2022**, *43*, 153.
57. D. Zhang, D. D. Arola, *J. Biomed. Opt.* **2004**, *9*, 691.
58. T. Luyckx, M. Verstraete, K. De Roo, W. De Waele, J. Bellemans, J. Victor, *J. Exp. Orthop.* **2014**, *1*, 1.
59. K. Holak, P. Kohut, M. Ekiert, K. Tomaszewski, T. Uhl, *Mech. Control.* **2015**, *34*, 19.
60. S. F. Kane, N. Carolina, C. Hill, N. Carolina, **2019**, *100*, 147.
61. E. Bass, *Int. J. Ther. Massage Bodywork* **2012**, *5*, 14.
62. N. L. Leong, F. A. Petrigliano, D. R. McAllister, *J. Biomed. Mater. Res., Part A* **2014**, *102*, 1614.
63. L. Huang, L. Chen, H. Chen, M. Wang, L. Jin, S. Zhou, L. Gao, R. Li, Q. Li, H. Wang, C. Zhang, J. Wang, *Biomimetics* **2023**, *8*, 246.
64. V. Franco, J. Grotts, J. C. Lin, M. K. Fong, M. S. Vasquez, *Muscles Ligaments Tendons J.* **2019**, *9*, 314.
65. I. Bousso, G. Genin, S. Thomopoulos, *Curr. Opin. Biomed. Eng.* **2024**, *31*, 100547.
66. V. Adukia, S. Jha, *Orthop. Trauma* **2024**, *38*, 11.
67. W. L. Lim, L. L. Liau, M. H. Ng, S. R. Chowdhury, J. X. Law, *Tissue Eng. Regener. Med.* **2019**, *16*, 549.
68. C. Vacanti, *J. Cell. Mol. Med.* **2006**, *1*, 569.
69. R. Langer, J. Vacanti, *J. Pediatr. Surg.* **2016**, *51*, 8.
70. X. Zhang, D. Bogdanowicz, C. Erisken, N. M. Lee, H. H. Lu, *J. Shoulder Elbow Surg.* **2012**, *21*, 266.
71. S. Sagadevan, R. Schirhagl, M. Z. Rahman, M. F. Bin Ismail, J. A. Lett, I. Fatimah, N. H. Mohd Kaus, W.-C. Oh, *J. Drug Delivery Sci. Technol.* **2023**, *82*, 104313.
72. T. Tawonsawatruk, A. Panaksri, R. Hemstapat, P. Praenet, K. Rattanapinyopituk, S. Boonyagul, N. Tanadchangsaeng, *Sci. Rep.* **2023**, *13*, 1.
73. F. Diaz, L. Zimmermann, T. P. Dale, N. R. Forsyth, A. R. Boccaccini, *Carbohydr. Polym. Technol. Appl.* **2024**, *7*, 100447.
74. S. Ruiz-Alonso, J. Ordoyo-Pascual, M. Lafuente-Merchan, I. Gallego, L. Sanchez-Del-Burgo, *Int. J. Bioprint* **2024**, *10*, 442.
75. S. Li, Y. Sun, Y. Chen, J. Lu, G. Jiang, K. Yu, Y. Wu, Y. Mao, H. Jin, J. Luo, S. Dong, B. Hu, Y. Ding, A. Liu, Y. Shen, G. Feng, S. Yan, Y. He, R. Yan, *ACS Appl. Mater. Interfaces* **2023**, *15*, 4652.
76. B. Shiroud Heidari, R. Ruan, E. Vahabli, P. Chen, E. De-Juan-Pardo, M. Zheng, B. Doyle, *Bioact Mater* **2023**, *19*, 179.
77. W. Wang, X. Lin, T. Tu, Z. Guo, Z. Song, Y. Jiang, B. Zhou, D. Lei, X. Wang, W. Zhang, G. Zhou, B. Yi, P. Zhang, W. Liu, *Biomater. Adv.* **2024**, *163*, 213950.
78. S. Bahrami, H. Mirzadeh, A. Solouk, D. Duprez, *Biotechnol. J.* **2023**, *18*, 2300117.
79. N. Turgut, F. Cengiz Çallıoğlu, A. Bayraktar, M. Savran, H. Aşçı, K. Gülle, M. Ünal, *Front. Surg.* **2024**, *11*, 1.
80. E. Reverchon, L. Baldino, S. Cardea, I. De Marco, *Muscles Ligaments Tendons J.* **2012**, *2*, 181.
81. A. R. Del Bakhshayesh, N. Asadi, A. Alihemmati, H. Tayefi Nasrbadi, A. Montaseri, S. Davaran, S. Saghati, A. Akbarzadeh, A. Abedelahi, *J. Biol. Eng.* **2019**, *13*, 1.
82. D. T. Govindaraju, C. H. Chen, K. T. Shalumon, H. H. Kao, J. P. Chen, *Nanomaterials* **2023**, *13*, 1847.
83. R. Sheng, Y. Jiang, L. J. Backman, W. Zhang, J. Chen, *Stem Cells Int.* **2020**, *2020*, 1.
84. D. W. Youngstrom, J. G. Barrett, *Stem Cells Int.* **2016**, *2016*, 3919030.
85. Y. Xu, Q. Wang, Y. Li, Y. Gan, P. Li, S. Li, Y. Zhou, Q. Zhou, *Biomed Res. Int.* **2015**, *2015*, 1.
86. Y. Qiu, J. Lei, T. J. Koob, J. S. Temenoff, *J. Tissue Eng. Regener. Med.* **2016**, *10*, 989.
87. L. A. Bosworth, S. R. Rathbone, R. S. Bradley, S. H. Cartmell, *J. Mech. Behav. Biomed. Mater.* **2014**, *39*, 175.
88. C. H. Lee, H. J. Shin, I. H. Cho, Y.-M. Kang, I. A. Kim, K.-D. Park, J.-W. Shin, *Biomaterials* **2005**, *26*, 1261.
89. K. Chen, Z. Liu, X. Zhou, W. Zheng, H. Cao, Z. Yang, Z. Wang, C. Ning, Q. Li, H. Zhao, *Biomater Res.* **2025**, *29*, 0132.
90. X. Lin, Y. Shi, Y. Cao, W. Liu, *Biomed. Mater.* **2016**, *11*, 014109.
91. J. S. Miller, J. A. Burdick, *ACS Biomater. Sci. Eng.* **2016**, *2*, 1658.
92. M. Rahmati, D. K. Mills, A. M. Urbanska, M. R. Saeb, J. R. Venugopal, S. Ramakrishna, M. Mozafari, *Prog. Mater. Sci.* **2021**, *117*, 100721.
93. S. Loewner, S. Heene, T. Baroth, H. Heymann, F. Cholewa, H. Blume, C. Blume, *Front. Bioeng. Biotechnol.* **2022**, *10*, 1.
94. G. Criscenti, A. Longoni, A. Di Luca, C. De Maria, C. A. VanBlitterswijk, G. Vozzi, L. Moroni, *Biofabrication* **2016**, *8*, 015009.
95. S. Zhong, Y. Lan, J. Liu, M. Seng Tam, Z. Hou, Q. Zheng, S. Fu, D. Bao, *J. Adv. Res.* **2025**, *67*, 361.
96. M. Kempfert, E. Willbold, S. Loewner, C. Blume, J. Pitts, H. Menzel, Y. Roger, A. Hoffmann, N. Angrisani, J. Reifenrath, *J. Funct. Biomater.* **2022**, *13*, 160.
97. M. R. Reinoso, M. Civera, V. Burgio, F. Bergamin, O. Grimaldo Ruiz, N. M. Pugno, C. Surace, *Acta Bioeng Biomech* **2021**, *23*, 63.
98. X. Jiang, S. Wu, M. Kuss, Y. Kong, W. Shi, PN Streubel, T. Li, B. Duan, *Bioact Mater* **2020**, *5*, 636.
99. H. Zhang, Z. Pei, C. Wang, M. Li, H. Zhang, J. Qu, *Tissue Eng., Part A* **2021**, *27*, 1343.
100. S. Wu, J. Liu, Y. Qi, J. Cai, J. Zhao, B. Duan, S. Chen, *Mater. Sci. Eng., C* **2021**, *126*, 112181.
101. T. Tu, Y. Shi, B. Zhou, X. Wang, W. Zhang, G. Zhou, X. Mo, W. Wang, J. Wu, W. Liu, *NPJ Regen. Med.* **2023**, *8*, 67.
102. S. Camarero-Espinosa, H. Yuan, P. J. Emans, L. Moroni, *Adv. Healthcare Mater.* **2023**, *12*, 2203023.
103. T. Tu, Y. Shen, X. Wang, W. Zhang, G. Zhou, Y. Zhang, W. Wang, W. Liu, *Appl. Mater. Today* **2020**, *18*, 100495.
104. D. Sheng, J. Li, C. Ai, S. Feng, T. Ying, X. Liu, J. Cai, X. Ding, W. Jin, H. Xu, J. Chen, S. Chen, *J. Mater. Chem. B* **2019**, *7*, 4801.
105. M. J. Baldwin, J. Y. Mimpen, A. P. Cribbs, E. Stace, M. Philpott, S. G. Dakin, A. J. Carr, S. J. B. Snelling, *Front. Bioeng. Biotechnol.* **2022**, *9*, 1.
106. Y. Song, L. Li, W. Zhao, Y. Qian, L. Dong, Y. Fang, L. Yang, Y. Fang, *Bioact Mater* **2021**, *6*, 2983.
107. X. Li, H. Chen, S. Xie, N. Wang, S. Wu, Y. Duan, M. Zhang, L. Shui, *Int. J. Nanomed.* **2020**, *15*, 6373.
108. H. M. Pauly, D. J. Kelly, K. C. Popat, N. A. Trujillo, N. J. Dunne, H. O. Mccarthy, T. L. Haut Donahue, *J. Mech. Behav. Biomed. Mater.* **2016**, *61*, 258.
109. H. Pauly, D. Kelly, K. Popat, J. Easley, R. Palmer, T. L. Haut Donahue, *J. Orthop. Res.* **2019**, *37*, 421.
110. S. Zhao, X. Zhao, S. Dong, J. Yu, G. Pan, Y. Zhang, J. Zhao, W. Cui, *J. Mater. Chem. B* **2015**, *3*, 990.

2688268x, 0, Downloaded from https://onlinelibrary.wiley.com/doi/10.1002/VIW.20250063 by CochraneItalia, Wiley Online Library on [16/10/2025]. See the Terms and Conditions (https://onlinelibrary.wiley.com/terms-and-conditions) on Wiley Online Library for rules of use; OA articles are governed by the applicable Creative Commons License

111. W. Su, Q. Yang, T. Li, J. Xu, P. Yin, M. Han, Z. Lin, Y. Deng, Y. Wu, W. Huang, L. Wang, *Small Methods* **2024**, *8*, 1.
112. M. von Witzleben, T. Stoppe, T. Ahlfeld, A. Bernhardt, M. L. Polk, M. Bornitz, M. Neudert, M. Gelinsky, *Adv. Healthcare Mater.* **2021**, *10*, 1.
113. G. Hochleitner, F. Chen, C. Blum, P. D. Dalton, B. Amsden, J. Groll, *Acta Biomater.* **2018**, *72*, 110.
114. J. Cai, J. Liu, J. Xu, Y. Li, T. Zheng, T. Zhang, K. Han, S. Chen, J. Jiang, S. Wu, J. Zhao, *Biofabrication* **2023**, *15*, 025002.
115. X. Xie, J. Xu, J. Lin, L. Chen, D. Ding, Y. Hu, K. Han, C. Li, F. Wang, J. Zhao, L. Wang, *Biofabrication* **2024**, *16*, 015018.
116. K. T. Shalumon, H.-T. Liao, W.-H. Li, D. T. G., M. P. A., J.-P. Chen, *Chem. Eng. J.* **2023**, *454*, 140366.
117. N. W. Pensa, A. S. Curry, P. P. Bonvallet, N. F. Bellis, K. M. Rettig, M. S. Reddy, A. W. Eberhardt, S. L. Bellis, *Biomater. Res.* **2019**, *23*, 1.
118. R. Alkaissy, M. Richard, H. Morris, S. Snelling, H. Pinchbeck, A. Carr, P.-A. Mouthuy, *Macromol. Biosci.* **2022**, *22*, 1.
119. S. Micalizzi, L. Russo, C. Giacomelli, F. Montemurro, C. D. Maria, M. Nencioni, L. Marchetti, M. L. Trincavelli, G. Vozzi, *Int. J. Bioprinting.* **2023**, *9*, 763.
120. K. Niveditha, A. John, J. Joseph, S. Mini, C. A. Vineeth, T. S. Swapna, A. Abraham, *J. Biomed. Mater. Res., Part B* **2023**, *111*, 1672.
121. J. Cui, Y.-J. Zhang, X. Li, J.-J. Luo, L.-L. Zhao, X.-Y. Xie, W. Ding, J.-C. Luo, T.-W. Qin, *J. Controlled Release* **2023**, *360*, 842.
122. X. Wang, K. Xu, L. Mu, X. Zhang, G. Huang, M. Xing, Z. Li, J. Wu, *Adv. Healthcare Mater*. **2023**, *12*, 1.
123. P. Chen, A. Wang, W. Haynes, E. Landao-Bassonga, C. Lee, R. Ruan, W. Breidahl, B. Shiroud Heidari, C. A. Mitchell, M. Zheng, *J. Orthop. Translat*. **2021**, *31*, 91.
124. A. Zaszczyńska, M. Moczulska-Heljak, A. Gradys, P. Sajkiewicz, *Materials* **2021**, *14*, 3149.
125. G. Wu, B. Sun, C. Zhao, Z. Wang, S. Teng, M. Yang, Z. Cui, G. Zhu, Y. Yu, *ACS Biomater. Sci. Eng.* **2021**, *7*, 5739.
126. C. Liang, Z. Fan, Z. Zhang, P. Wang, H. Deng, J. Tao, *RSC Adv.* **2024**, *14*, 26077.
127. R. Di Gesù, G. Amato, R. Gottardi, *Muscles Ligaments Tendons J.* **2019**, *9*, 478.
128. O. Evrova, G. M. Bürgisser, C. Ebnöther, A. Adathala, M. Calcagni, E. Bachmann, J. G. Snedeker, C. Scalera, P. Giovanoli, V. Vogel, J. Buschmann, *Biomaterials* **2020**, *232*, 119722.
129. M. B. Guner, A. D. Dalgic, A. Tezcaner, S. Yilanci, D. Keskin, *Biomed Mater* **2020**, *15*, 065014.
130. D. T. G., C.-H. Chen, C.-Y. Kuo, K. T. Shalumon, Y.-M. Chien, H.-H. Kao, J.-P. Chen, *Int. J. Biol. Macromol.* **2022**, *221*, 314.
131. H. Xuan, Z. Zhang, W. Jiang, N. Li, L. Sun, Y. Xue, H. Guan, H. Yuan, *Colloids Surf., B* **2023**, *228*, 113416.
132. D. A. Brennan, A. A. Conte, G. Kanski, S. Turkula, X. Hu, M. T. Kleiner, V. Beachley, *Adv. Healthcare Mater.* **2018**, *7*, 1.
133. P. A. Mouthuy, N. Zargar, O. Hakimi, E. Lostis, A. Carr, *Biofabrication* **2015**, *7*, 025006.
134. S. Font Tellado, E. R. Balmayor, M. Van Griensven, *Adv. Drug Delivery Rev.* **2015**, *94*, 126.
135. Z. Mao, B. Fan, X. Wang, X. Huang, J. Guan, Z. Sun, B. Xu, M. Yang, Z. Chen, D. Jiang, J. Yu, *Front. Bioeng. Biotechnol.* **2021**, *9*, 621483.
136. L. Weidenbacher, A. Abrishamkar, M. Rottmar, A. G. Guex, K. Maniura-Weber, A. J. Demello, S. J. Ferguson, R. M. Rossi, G. Fortunato, *Acta Biomater.* **2017**, *64*, 137.
137. A. Hrynevich, B. Ş. Elçi, J. N. Haigh, R. Mcmaster, A. Youssef, C. Blum, T. Blunk, G. Hochleitner, J. Groll, P. D. Dalton, *Small* **2018**, *14*, 1.
138. P. G. Saiz, A. Reizabal, J. L. Vilas-Vilela, P. D. Dalton, S. Lanceros-Mendez, *Adv. Mater.* **2024**, *36*, 1.
139. M. von Witzleben, J. Hann, R. F. Ritcher, B. de Freitas, E. Steyer, K. Schütz, C. Vater, A. A. Bernhardt, C. Elschner, M. Gelinsky, *Biomater. Adv.* **2024**, *156*, 213708.
140. Y. Han, B. Jia, M. Lian, B. Sun, Q. Wu, B. Sun, Z. Qiao, K. Dai, *Bioact Mater* **2021**, *6*, 2173.
141. Y. Yin, H. Yang, W. Han, C. Guo, Q. Mu, H. Yang, D. Chen, *Polym. Adv. Technol.* **2025**, *36*, e70067.
142. O. Vesvoranan, A. Anup, K. R. Hixon, *Biomimetics* **2022**, *7*, 151.
143. G. D. Learn, P. E. Mcclellan, D. M. Knapik, J. L. Cumsky, V. Webster-Wood, J. M. Anderson, R. J. Gillespie, O. Akkus, *J. Biomed. Mater. Res., Part B* **2019**, *107*, 1864.
144. A. Jayasree, S. Kottappally Thankappan, R. Ramachandran, M. N. Sundaram, C.-H. Chen, U. Mony, J.-P. Chen, R. Jayakumar, *ACS Biomater. Sci. Eng.* **2019**, *5*, 1476.
145. M. Laranjeira, R. M. A. Domingues, R. Costa-Almeida, R. L. Reis, M. E. Gomes, *Small* **2017**, *13*, 1.
146. Y. H. Tan, H. R. Helms, K. H. Nakayama, *Front. Bioeng. Biotechnol.* **2022**, *10*, 1.
147. L.-J. Ning, J. Cui, S.-K. He, R.-N. Hu, X. Yao, Y. Zhang, W. Ding, Y.-J. Zhang, J.-C. Luo, T.-W. Qin, *Regen. Biomater.* **2022**, *9*, rbac020.
148. A. Dede Eren, R. Sinha, E. Deniz Eren, Y. Huipin, S. Gulce-Iz, H. Valster, L. Moroni, J. Foolen, J. de Boer, *J. Immunol. Regen Med.* **2020**, *8*, 100027.
149. S. Chae, Y. J. Choi, D. W. Cho, *Biofabrication* **2022**, 14, 025013.
150. R. Mhanna, A. Hasan, in (Eds: A. Hasan), *Tissue Engineering For Artificial Organs: Regenerative Medicine, Smart Diagnostics and Personalized Medicine*, Elsevier, Amsterdam **2017**, 1.
151. M. Young, *Stem Cells Int*. **2012**, *2012*, 1.
152. B. P. Roßbach, M. F. Gülecyüz, L. Kempfert, M. F. Pietschmann, T. Ullamann, A. Ficklscherer, T. R. Niethammer, A. Zhang A, R. M. Klar, P. E. Müller, *Am. J Sports Med.* **2020**, *48*, 450.
153. M. Beldjilali-Labro, A. Garcia Garcia, F. Farhat, F. Bedoui, J.-F. Grosset, M. Dufresne, C. Legallais, *Materials* **2018**, *11*, 1116.
154. M. Li, Y. Wu, T. Yuan, H. Su, M. Qin, X. Yang, S. Mi, *ACS Appl. Mater. Interfaces* **2023**, *15*, 47989.
155. S. Yang, X. Shi, X. Li, J. Wang, Y. Wang, Y. Luo, *Biomaterials* **2019**, *207*, 61.
156. B. Bauer, C. Emonts, J. Pitts, E. M. Buhl, J. Eschweiler, R. Hänsch, M. Betsch, T. Gries, H. Menzel, *Polymers* **2024**, *16*, 488.
157. Y. Li, Z. Ge, Z. Liu, L. Li, J. Song, H. Wang, F. Tian, P. Lei, L. Li, J. Xue, *J. Nanobiotechnol.* **2024**, *22*, 1.
158. M. Sriram, S. Priya, A. Mahajan, D. S. Katti, *Biofabrication* **2024**, *16*, 025015.
159. T. Später, et al., *Front. Bioeng. Biotechnol.* **2024**, *12*, 1.
160. W. Kim, G.-E. Kim, M. Attia Abdou, S. Kim, D. Kim, S. Park, Y.-K. Kim, Y. Gwon, S.-E. Jeong, M.-S. Kim, J. Kim, *ACS Omega* **2020**, *5*, 13913.
161. Y. Maghdouri-White, N. Sori, S. Petrova, H. Wriggers, N. Kemper, A. Dasgupta, K. Coughenour, S. Polk, N. Thayer, M.

2688268x, 0, Downloaded from https://onlinelibrary.wiley.com/doi/10.1002/VIW.20250063 by CochraneItalia, Wiley Online Library on [16/10/2025]. See the Terms and Conditions (https://onlinelibrary.wiley.com/terms-and-conditions) on Wiley Online Library for rules of use; OA articles are governed by the applicable Creative Commons License

Rodriguez, B. Simon, A. Bulysheva, K. Bonner, S. Arnoczky, S. Adams, M. P. Francis, *Biomed. Mater.* **2021**, *16*, 025025.
162. W. Lun, H. Wang, M. Li, J. Ma, Y. Ding, X. Zheng, X. Cao, Q. Li, *Adv. Healthcare Mater*. **2025**, *14*, 1.
163. C. Emonts, B. Bauer, C. Büchter, T. Pufe, T. Gries, M. Tohidnezhad, *Int. J. Mol. Sci.* **2025**, *26*, 1735.
164. C. Meyers, J. Lisiecki, S. Miller, A. Levin, L. Fayad, C. Ding, T. Sono, E. Mccarthy, B. Levi, A. W. James, *JBMR Plus* **2019**, *3*, e10172.
165. P. Dec, M. Żyłka, P. Burszewski, A. Modrzejewski, A. Pawlik, *Int. J. Mol. Sci.* **2024**, *25*, 4498.
166. Y. Bi, D. Ehirchiou, T. M. Kilts, C. A. Inkson, M. C. Embree, W. Sonoyama, L. Li, A. I. Leet, B.-M. Seo, L. Zhang, S. Shi, M. F. Young, *Nat. Med.* **2007**, *13*, 1219.
167. J. Yang, Q. Zhao, K. Wang, H. Liu, C. Ma, H. Huang, Y. Liu, *In Vitro Cell. Dev. Biol. Anim.* **2016**, *52*, 846.
168. F. Qi, Z. Deng, Y. Ma, S. Wang, C. Liu, F. Lyu, T. Wang, Q. Zheng, *Ann. Transl. Med.* **2020**, *8*, 131.
169. A. W. Clarke, F. Alyas, T. Morris, C. J. Robertson, J. Bell, D. A. Connell, *Am. J. Sports Med.* **2011**, *39*, 614.
170. S. E. DiIorio, B. Young, J. B. Parker, M. F. Griffin, M. T. Longaker, *Biomedicines* **2024**, *12*, 859.
171. Y. H. Son, D. H. Yang, B. Uricoli, S.-J. Park, G.-J. Jeong, H. J. Chun, *Tissue Eng. Regener. Med.* **2023**, *20*, 553.
172. C. Ning, P. Li, C. Gao, L. Fu, Z. Liao, G. Tian, H. Yin, M. Li, X. Sui, Z. Yuan, S. Liu, Q. Guo, *Front. Bioeng. Biotechnol.* **2023**, *11*, 1.
173. G. Lutzweiler, A. Ndreu Halili, N. Engin Vrana, *Pharmaceutics* **2020**, *12*, 602.
174. D. M. Ramos, S. Abdulmalik, M. R. Arul, N. Sardashti, Y. K. Banasavadi-Siddegowda, S. P. Nukavarapu, H. Drissi, S. G. Kumbar, *ACS Appl. Bio Mater.* **2022**, *5*, 2851.
175. S. Abdulmalik, J. Gallo, J. Nip, S. Katebifar, M. Arul, A. Lebaschi, L. N. Munch, J. M. Bartly, S. Choudhary, I. Kalajzic, Y. K. Banasavadi-Siddegowdae, S.P Nukavarapu, S. G. Kumbar, *Bioact Mater* **2023**, *25*, 42.
176. M. Silva, S. Gomes, C. Correia, D. Peixoto, A. Vinhas, M. T. Rodrigues, M. E. Gomes, J. A. Covas, M. C. Paiva, N. M. Alves, *Nanomaterials* **2023**, *13*, 2518.
177. C. Rinoldi, E. Kijeńska-Gawrońska, M. Heljak, J. Jaroszewicz, A. Kamiński, A. Khademhosseini, A. Tamayol, W. Swieszkowski, *ACS Materials Au* **2023**, *3*, 636.
178. I. Donderwinkel, R. S. Tuan, N. R. Cameron, J. E. Frith, *J. Orthop Translat.* **2023**, *43*, 1.
179. I. M. Adel, M. F. ElMeligy, M. S. Amer, N. A. Elkasabgy, *Eur. J. Pharm. Sci.* **2024**, *192*, 106659.
180. Y.-H. Yu, C.-H. Lee, Y.-H. Hsu, Y.-C. Chou, P.-C. Yu, S.-J. Liu, *Macromol. Mater. Eng.* **2023**, *308*, 1.
181. N. Pien, Y. Van De Maele, L. Parmentier, M. Meeremans, A. Mignon, C. De Schauwer, I. Peeters, L. De Wilde, A. Martens, D. Mantovani, S. Van Vlierberghe, P. Dubruel, *J. Mater. Sci.: Mater. Med.* **2022**, *33*, 51.
182. M. Zuhour, C. Günes, S. Findik, M. A. Dündar, O. Gök, Z. Altuntaş, *J. Drug Deliv. Sci. Technol.* **2023**, *89*, 104988.
183. K. Duan, Z. Ling, M. Sun, W. Zhi, Y. Zhang, S. Han, J. Xu, H. Wang, J. Li, *J. Appl. Polym. Sci.* **2022**, *139*, 1.
184. A. B. R. Touré, E. Mele, J. K. Christie, *Nanomaterials* **2020**, *10*, 1.
185. Y. J. No, S. Tarafder, B. Reischl, Y. Ramaswamy, C. Dunstan, O. Friedrich, C. H. Lee, H. Zreiqat, *ACS Biomater. Sci. Eng.* **2020**, *6*, 1887.
186. Y. L. Zhou, Q. Q. Yang, Y. Y. Yan, C. Zhu, L. Zhang, J. B. Tang, *Acta Biomater.* **2018**, *70*, 237.
187. Y. Zhou, L. Zhang, W. Zhao, Y. Wu, C. Zhu, Y. Yang, *Biomaterials* **2013**, *34*, 8269.
188. F. Zhou, X. Jia, Y. Yang, Q. Yang, C. Gao, S. Hu, Y. Zhao, Y. Fan, X. Yuan, *Acta Biomater.* **2016**, *43*, 303.
189. Z. Yao, J. Li, X. Wang, S. Peng, J. Ning, Y. Qian, C. Fan, *J. Inflamm. Res.* **2020**, *13*, 303.
190. Z. Ren, Z. Duan, Z. Zhang, R. Fu, C. Zhu, D. Fan, *Int. J. Biol. Macromol.* **2023**, *242*, 125001.
191. P. Santoro Belangero, E. Antônio Figueiredo, C. Cohen, F. De Seixas Alves, W. Hiromi Yanaguizawa, M. Cardoso Smith, C. Vicente Andreoli, A. De Castro Pochini, M. Teresa De Seixas Alves, B. Ejnisman, M. Cohen, M. Ferreira Leal, *J. Orthop. Res.* **2018**, *36*, 2542.
192. Y. Li, X. Liu, X. Liu, Y. Peng, B. Zhu, S. Guo, C. Wang, D. Wang, S. Li, *Groundwater* **2022**, *40*, 98.
193. R. Di Gesù, A. P. Piccionello, G. Vitale, S. Buscemi, S. Panzavolta, M. F. Di Filippo, A. Leonarda, M. Cuccia, A. Di Prima, R. Gottardi, *Biofabrication* **2025**, *17*, 025025.
194. T. Katagiri, T. Watabe, *Cold Spring Harbor Perspect. Biol*. **2016**, *8*, a021899.
195. Z. Yuan, H. Yu, H. Long, Y. Dai, L. Shi, J. Zhao, A. Guo, N. Diao, L. Ma, H. Yin, *Stem Cells Int.* **2023**, *2023*, 1.
196. M. Majewski, P. Heisterbach, C. Jaquiéry, L. Dürselen, A. Todoro, I. Martin, C. H. Evans, S. A. Müller, *Eur. Cells Mater.* **2018**, *35*, 318.
197. X. Liu, Y. Li, S. Wang, M. Lu, J. Zou, Z. Shi, B. Xu, W. Wang, B. Hu, T. Jin, F. Wu, S. Liu, C. Fan, *Mater Today Bio.* **2022**, *16*, 1.
198. A. Bedi, T. Maak, C. Walsh, S. A. Rodeo, D. Grande, D. M. Dines, J. S. Dines, *J. Shoulder Elbow Surg.* **2012**, *21*, 218.
199. Y. Zeng, J. Hoque, S. Varghese, *Acta Biomater.* **2019**, *93*, 152.
200. A. Zielińska, J. Karczewski, P. Eder, T. Kolanowski, M. Szalata, K. Wielgus, M. Szalata, D. Kim, S. R. Shin, R. Słomski, E. B. Souto, *J. Controlled Release* **2023**, *359*, 207.
201. Y. C. Chen, S. F. Gad, D. Chobisa, Y. Li, Y. Yeo, *J. Controlled Release* **2021**, *330*, 438.
202. T. Peixoto, M. C. Paiva, A. T. Marques, M. A. Lopes, *Adv. Eng. Mater.* **2020**, *22*, 1.
203. A. K. Badekila, S. Kini, A. K. Jaiswal, *J. Cell. Physiol.* **2021**, *236*, 741.
204. M. Cannio, D. Bellucci, J. A. Roether, D. N. Boccaccini, V. Cannillo, *Materials* **2021**, *14*, 5440.
205. J. R. Jones, D. S. Brauer, L. Hupa, D. C. Greenspan, *Int. J. Appl. Glass Sci.* **2016**, *7*, 423.
206. J. A. Spadair, R. O. Becker, C. H. Bachman, Calcified Tissue Research **1970**, *6*, 49.
207. G. M. Kuang, W. P. Yau, W. W. Lu, K. Y. Chiu, *Am. J. Sports Med.* **2014**, *42*, 2996.
208. L. Giordano, G. D. Porta, G. M. Peretti, N. Maffulli, *Br. Med. Bull.* **2020**, *133*, 79.
209. C. J. P. Silva, E. R. Balmayor, M. van Griensven, *Front. Bioeng. Biotechnol.* **2024**, *12*, 1.
210. S. W. L. Lee, C. Paoletti, M. Campisi, T. Osaki, G. Adriani, R. D. Kamm, C. Mattu, V. Chiono, *J. Controlled Release* **2019**, *313*, 80.

2688268x, 0, Downloaded from https://onlinelibrary.wiley.com/doi/10.1002/VIW.20250063 by CochraneItalia, Wiley Online Library on [16/10/2025]. See the Terms and Conditions (https://onlinelibrary.wiley.com/terms-and-conditions) on Wiley Online Library for rules of use; OA articles are governed by the applicable Creative Commons License

211. F. C. Moraes, C. Pichon, D. Letourneur, F. Chaubet, *Pharmaceutics* **2021**, *13*, 1901.
212. Q. Liu, Y. Zhu, W. Zhu, G. Zhang, Y. P. Yang, C. Zhao, *Biomaterials* **2021**, *277*, 121083.
213. K. Lyu, X. Liu, T. Liu, J. Lu, L. Jiang, Y. Chen, L. Long, X. Wang, H. Shi, F. Wang, S. Li, *Cell Tissue Res.* **2023**, *393*, 201.
214. M. Bottagisio, A. B. Lovati, *J. Mater. Sci.: Mater. Med.* **2017**, *28*, 45.
215. M. T. Rodrigues, R. L. Reis, M. E. Gomes, *J Tissue Eng Regen Med*. **2013**, *7*, 673.
216. D. Little, P. C. Amadio, H. A. Awad, S. G. Cone, N. A. Dyment, M. B. Fisher, A. H. Huang, D. W. Koch, A. F. Kuntz, R. Madi, K. Mcgilvray, L. V. Schnabel, S. S. Shetye, S. Thomopoulos, C. Zhao, L. J. Soslowsky, *J. Orthop. Res.* **2023**, *41*, 2133.
217. S. S. Novakova, V. D. Mahalingam, S. E. Florida, C. L. Mendias, A. Allen, E. M. Arruda, A. Bedi, L. M. Larkin, *J. Orthop. Res.* **2018**, *36*, 289.
218. Q. Shi, H. Wang, K. He, M. Tao, C. K. Cheng, *Front. Vet. Sci.* **2022**, *9*, 1045785.
219. G. Zhang, X. Zhou, S. Hu, Y. Jin, Z. Qiu, *Front. Cell Dev. Biol.* **2022**, *10*, 1.

How to cite this article: F. Romano, F. Lopresti, R. D. Gesù, V. La Carrubba, *VIEW*. **2025**, 20250063. https://doi.org/10.1002/VIW.20250063

AUTHOR BIOGRAPHIES

Francesca Romano is a second-year PhD student in Chemical, Environmental, Biomedical, Hydraulic and Materials Engineering at the University of Palermo. She obtained a Bachelor's Degree in Biomedical Engineering (Biomaterials and Medical Devices) in October 2021 and a Master's Degree in Biomedical Engineering (Biomaterials for Regenerative Medicine) in October 2023, both from the University of Palermo. Her doctoral research is jointly carried out at the Bio and Tissue Engineering Laboratory of the University of Palermo and the Musculoskeletal Tissue Engineering (MsTE) group at Fondazione Ri.MED, with a focus on the development of bioactive scaffolds capable of providing proregenerative signals to musculoskeletal tissues. More specifically, her project aims at designing smart, bioactive, and implantable 3D porous scaffolds to mimic natural tendons and promote their healing. These scaffolds, fabricated from FDA-approved materials, are engineered to replicate the structural and functional properties of human tendons, with the goal of improving treatments for both traumatic and degenerative tendon injuries. She is about to begin an international research period at the MERLN Institute for Technology-Inspired Regenerative Medicine (Maastricht University, The Netherlands).

Dr Roberto Di Gesù is the Principal Investigator of the Musculoskeletal Tissue Engineering Laboratory at the Ri.MED Foundation, a leading biomedical and biotechnology research hub located in Palermo, Italy. With a rich career blending academic and industry experience, he has given significant advances to the fields of tissue engineering, drug delivery, and therapeutic innovation. Roberto began his journey with a degree from Pharmacy School, followed by a PhD in Biotechnology from the University of Palermo, where he explored bone tissue engineering and drug delivery systems for cancer and Alzheimer's disease. During his first postdoctoral role at the Italian National Research Council (CNR) he developed an innovative polymeric drug delivery system for the maculopathy treatment. Later, as a Senior Scientist at Merck in Rome, he played a key role in developing Bavencio, an anticancer monoclonal antibody now available in the US market. Passionate about academic research, Roberto took on a second postdoctoral position at the University of Bologna, focusing on electrospun drug delivery systems for spinal cord injuries. Through Ri.MED's global partnerships, he has also been a visiting research scientist at two top US institutions such as the University of Pittsburgh and the Children's Hospital of Philadelphia. At Ri.MED, Roberto now leads pioneering efforts to create 3D in vitro models to study musculoskeletal disorders and develop new treatment approaches. His work continues to push the boundaries of regenerative medicine, aiming to improve outcomes for patients with complex conditions.

2688268x, 0, Downloaded from https://onlinelibrary.wiley.com/doi/10.1002/VIW.20250063 by CochraneItalia, Wiley Online Library on [16/10/2025]. See the Terms and Conditions (https://onlinelibrary.wiley.com/terms-and-conditions) on Wiley Online Library for rules of use; OA articles are governed by the applicable Creative Commons License